

## INFORMATION TO USERS

This material was produced from a microfilm copy of the original document. While the most advanced technological means to photograph and reproduce this document have been used, the quality is heavily dependent upon the quality of the original submitted.

The following explanation of techniques is provided to help you understand markings or patterns which may appear on this reproduction.

1. The sign or "target" for pages apparently lacking from the document photographed is "Missing Page(s)". If it was possible to obtain the missing page(s) or section, they are spliced into the film along with adjacent pages. This may have necessitated cutting thru an image and duplicating adjacent pages to insure you complete continuity.
2. When an image on the film is obliterated with a large round black mark, it is an indication that the photographer suspected that the copy may have moved during exposure and thus cause a blurred image. You will find a good image of the page in the adjacent frame.
3. When a map, drawing or chart, etc., was part of the material being photographed the photographer followed a definite method in "sectioning" the material. It is customary to begin photoing at the upper left hand corner of a large sheet and to continue photoing from left to right in equal sections with a small overlap. If necessary, sectioning is continued again – beginning below the first row and continuing on until complete.
4. The majority of users indicate that the textual content is of greatest value, however, a somewhat higher quality reproduction could be made from "photographs" if essential to the understanding of the dissertation. Silver prints of "photographs" may be ordered at additional charge by writing the Order Department, giving the catalog number, title, author and specific pages you wish reproduced.
5. PLEASE NOTE: Some pages may have indistinct print. Filmed as received.

**Xerox University Microfilms**

300 North Zeeb Road  
Ann Arbor, Michigan 48106

75-18,707

BAYEWITZ, Marvin Herbert, 1947-  
GROWTH OF PARTICLES IN COALESCING SYSTEMS.

The City University of New York, Ph.D., 1975  
Engineering, chemical

**Xerox University Microfilms**, Ann Arbor, Michigan 48106

**GROWTH OF PARTICLES IN COALESCING SYSTEMS**

by

**MARVIN H. BAYEWITZ**

A dissertation submitted to the Graduate Faculty in  
Engineering in partial fulfillment of the requirements for the  
degree of Doctor of Philosophy, The City University of New York.

1975

This manuscript has been read and accepted for the Graduate Faculty in Engineering in satisfaction of the dissertation requirement for the degree of Doctor of Philosophy.

4/23/75  
date

Paul Blum  
Chairman of Examining Committee

4/23/75  
date

Jacques E. Benveniste  
Executive Officer

Prof. Robert Pfeffer

Prof. Frederick E. Thau

Prof. Joseph Yerushalmi

The City University of New York

## ABSTRACT

In the first part of this thesis an examination is made of the validity of a kinetic equation widely used in the literature in studying coalescing systems. A stochastic model of coalescence is set up and solved for the probabilities of all possible histories of particle growth. The full stochastic model is compared with the so-called kinetic model to which it reduces in the absence of correlations. A primary objective is the assesment of the extent of correlations in poorly mixed systems or in systems of small populations. The study shows that insofar as the total number of particles is concerned, regardless of their size distribution, the results from the kinetic equations match the true stochastic averages even for very small initial populations. But, when size distributions are considered, then, in systems of small population or in large systems that are poorly mixed, the results of the kinetic equations may differ substantially from the stochastic means in the long-term tail; apart from the tail, the distributions from the full stochastic and kinetic

models match quite well.

In the second part of this thesis kinetic equations of the type previously studied are used in a model which stimulates the evolution of seeded supercooled stationary clouds. The model contains mass balances on the inventories of solid, liquid and vapor in the cloud and embodies six microphysical processes affecting the distributions of ice particles and water drops. Solutions are obtained for the first three moments of the distributions using constant as well as sum-of-the-masses coefficients. The effects of various parameters on the evolution of seeded clouds are discussed. Seeding is found to have a significant effect on particle growth in continental clouds. The optimum seeding concentration is determined to be of the same order as the initial concentration of water drops.

## DEDICATION

This thesis is dedicated to my wonderful parents who enabled me to have the opportunities which they never had. It is also dedicated to the memory of Aharon Kestenbaum, who was my closest friend in graduate school and who was killed on October 24, 1973 fighting for the State of Israel in the Yom Kippur War.

## ACKNOWLEDGEMENTS

I wish to thank Professor Reuel Shinnar, who directed this research, and Professor Joseph Yerushalmi for their continuous guidance and their many contributions.

I wish to acknowledge the help of the late Professor Stanley Katz, my original mentor, who was instrumental in getting the research started.

During my research I was supported by a National Science Foundation Traineeship. This support is gratefully acknowledged.

## TABLE OF CONTENTS

	<u>Page</u>
ABSTRACT.....	ii
LIST OF FIGURES.....	viii
NOMENCLATURE.....	xiii
CHAPTER 1. INTRODUCTION.....	1
1.1 Preliminary Remarks.....	1
1.2 Aim and Scope of the Thesis.....	3
CHAPTER 2. THE EXTENT OF CORRELATIONS IN A STOCHASTIC COALESCENCE PROCESS.....	4
2.1 Introduction.....	4
2.2 Formulation of the Stochastic Model.....	8
2.3 The Kinetic Equations.....	13
2.4 Solutions I: The Total Number of Particles.	17
2.5 Solutions II: The Size Spectrum.....	29
2.6 Correlations in Poorly-Mixed Systems.....	33
2.7 Conclusions.....	42
CHAPTER 3. THE EFFECT OF SEEDING ON PARTICLE GROWTH IN SUPERCOOLED CLOUDS.....	45
3.1 Introduction.....	45
3.2 Formulation of the Model.....	50
3.3 Choice of the Collection Coefficient.....	57
3.4 The Dimensionless Equations.....	60

TABLE OF CONTENTS (continued)

	<u>Page</u>
3.5 The Moment Equations .....	64
3.6 Solutions - Constant Collection Coefficients ..	76
3.7 Solutions - Sum-of-the-Masses Coefficients ....	86
3.8 The Effects of Temperature Changes During Glaciation .....	92
3.9 Conclusions .....	97
APPENDIX A .....	99
APPENDIX B .....	105
BIBLIOGRAPHY .....	109
VITA .....	114

## LIST OF FIGURES

<u>Figure</u>	<u>Page</u>
2.1 $\langle N \rangle$ and $N$ as functions of $Ct$ . $\langle N \rangle$ is given by eq. (2.35) and $N$ by eq. (2.36).	20
2.2 The variance, $\sigma^2$ , and the mean, $\langle N \rangle$ , as functions of $Ct$ . $N_0 = 20$ .	22
2.3 $\sigma^2 / \langle N \rangle$ for a Poisson initial distribution with $\langle N_0 \rangle = 20$ .	25
2.4a $v_N(t)$ when $\langle N \rangle = 8.9$ ( $\langle N_0 \rangle = 20$ , $Ct = 0.125$ ) compared to the Poisson distribution with the same mean.	26
2.4b $v_N(t)$ when $\langle N \rangle = 8.9$ ( $\langle N_0 \rangle = 20$ , $Ct = 0.125$ ) compared to the Poisson distribution with the same mean.  (Continuous version of Fig.2.4a.)	27
2.5 The mean number of particles arising from a uniform initial distribution and from a Poisson initial distribution. $\langle N_0 \rangle = 20$ .	28
2.6 $P(n, 2; t)$ and Poisson distribution with the same mean at three successive values of $Ct$ . $N_0 = 20$ .	31

LIST OF FIGURES (continued)

<u>Figure</u>	<u>Page</u>
2.7 $P(n,5;t)$ and Poisson distribution with the same mean at three successive values of $Ct$ . $N_0 = 20$ .	32
2.8    Comparison between the stochastic concentration, $\langle f \rangle$ , and the deterministic concentration, $f$ , in a partitioned volume. $f_0 = 100$ . $N_0 = 10, 50, 100$ .	35
2.9    Mass fraction distribution at $Kt = .01$ .	39
2.10    Mass fraction distribution at $Kt = .02$ .	40
2.11    Mass fraction distribution at $Kt = .04$ .	41
3.1 $F(100\mu, \tau)$ vs. dimensionless time, $\tau$ , for different values of $\psi$ . Constant collection coefficients are in use, and $a_B(t,0) = 0.2$ . $A(T,0) = 0$ , $\beta = 1.0$ and $\nu = 1.0$	77
3.2    Dimensionless time for $F(100\mu, \tau)$ to reach 0.6 as a function of $\psi$ . Constant collection coefficients are in use, and $\beta = 1, \nu = 1, A(T,0) = 0$ .	79

LIST OF FIGURES (continued)

<u>Figure</u>	<u>Page</u>
3.3 The time, $t_{0.6}$ , for $F(100\mu, \tau)$ to reach 0.6 as a function of the seeding concentration. Constant collection coefficients are in use and $N_0 = 3.5 \times 10^7 \text{ m}^{-3}$ . $\beta = 1, \nu = 1, A(T,0) = 0$ .	80
3.4 Seeding efficiency vs. $\alpha B(T,0)$ . Constant collection coefficients are in use and $\beta = 1, \nu = 1, A(T,0) = 0$ .	82
3.5 Dimensionless time, $\tau_{0.6}$ , for $F(100\mu, \tau)$ to reach 0.6 as a function of $\psi$ for three values of $\beta$ . Constant collection coefficients were used, and $\alpha B(T,0) = 0.2, \nu=1, A(T,0) = 0$ .	84
3.6 Dimensionless time, $\tau_{0.6}$ , for $F(100\mu, \tau)$ to reach 0.6 as a function of $\psi$ for three values of $\nu$ . Constant collection coefficients are in use, and $\alpha B(T,0) = 0.2, A(T,0) = 0. \beta = 0$ .	85
3.7 The time, $t_{0.6}$ , for $F(100\mu, \tau)$ to reach 0.6 as a function of the seeding level. Sum-of-the-masses coefficients are in use and $N_0 = 4.22 \times 10^8 \text{ m}^{-3}$ . $E_H = E_R = 1. A(T,0) = 0$ . When $n_f \rightarrow \infty$ , $t_{0.6}$ approaches 950 sec. for $\alpha B(T,0) = 40$ , and 490 sec. for $\alpha B(T,0) = 20$ .	88

LIST OF FIGURES (continued)

<u>Figure</u>	<u>Page</u>
<p>3.8 The time, <math>t_{0.6}</math>, for <math>F(100\mu, \tau)</math> to reach 0.6 as a function of the seeding level for the maritime cloud and for continental cloud I. Sum-of-the-masses coefficients are in use and <math>\alpha_B(T,0) = 5.5</math> for the maritime cloud. <math>\alpha_B(T,0) = 20</math> for continental cloud I. <math>E_H = E_R = 1</math>. <math>A(T,0) = 0</math>.</p>	89
<p>3.9 Dimensionless time, <math>\tau_{0.6}</math>, for <math>F(100\mu, \tau)</math> to reach 0.6 as a function of <math>\psi</math> for continental clouds I and II. Sum-of-the-masses coefficients are used and <math>\alpha_B(T,0) = 40</math>. <math>E_H = E_R = 1</math>. <math>A(T,0) = 0</math>. As <math>\psi \rightarrow \infty</math> <math>\tau_{0.6}</math> approaches 3.0 and 2.75 for clouds I and II, respectively.</p>	91
<p>3.10 Dimensionless time, <math>\tau_{0.6}</math>, for <math>F(100\mu, \tau)</math> to reach 0.6 as a function of <math>\psi</math> for continental cloud I under isothermal and nonisothermal conditions. Sum-of-the-masses coefficients are in use and <math>\alpha_B(T,0) = 20</math>, <math>A(T,0) = 0</math>, <math>E_H = E_R = 1</math>. As <math>\psi \rightarrow \infty</math> <math>\tau_{0.6}</math> tends to 3.0 and 3.15 for the isothermal and the nonisothermal clouds, respectively.</p>	94

LIST OF FIGURES (continued)

<u>Figure</u>		<u>Page</u>
3.11	$\rho, \rho_w$ and $\rho_H$ vs. % glaciation for the nonisothermal cloud of Fig. 3.10.	95
3.12	Per cent glaciation at $\tau = \tau_{0.6}$ as a function of $\Psi$ for the nonisothermal cloud of Fig. 3.10.	96

## NOMENCLATURE

$A(T, \tau)$	.....	Dimensionless term defined in eq. (3.16)
$B(T, \tau)$	.....	Dimensionless term defined in eq. (3.16)
$b$	.....	Constant, see eq. (3.15)
$b'$	.....	$b/\rho_i$
$C$	.....	Collection coefficient
$D$	.....	Diffusivity of vapor in air
$D_p$	.....	Diffusivity of silver iodide particles in air
$E$	.....	Entrapment coefficient
$F(100\mu, \tau)$	.....	Fraction of available mass present in particles having radius greater than $100\mu$ at time $\tau$ .
$f(m, t)$	.....	$x_m(t)/V$
$f_0$	.....	Concentration of unit-size particles at $t=0$
$f$	.....	$N/V$
$G(T, t)$	.....	Dimensional term defined by eq. (3.9)
$H(m, t)$	.....	Distribution of ice particles
$h(y, \tau)$	.....	Dimensionless distribution of ice particles
$K(m, m')$	.....	Collection coefficient

NOMENCLATURE (continued)

$K$ .....	CV
$M_0$ .....	Initial water droplet mass concentration
$N$ .....	Total number of particles in a system or in a compartment from the kinetic model
$\langle N \rangle$ .....	Stochastic mean number of particles in a system or in a compartment
$N_0$ .....	Initial population size in a system or in a compartment
$n_f$ .....	Number concentration of silver iodide particles
$P(n,m;t)$ .....	Probability of having exactly $n$ particles of size $m$ at time $t$
$p_w(T)$ .....	Vapor pressure around water droplet
$Q$ .....	Constant of contact nucleation
$T$ .....	Temperature
$U(T,t)$ .....	Dimensional term defined in eq. (3.12)
$v(N, x_1, x_2, \dots; t)$ .....	Probability associated with the indicated distribution
$v_N(t)$ .....	Probability of having $N$ particles of whatever size

## NOMENCLATURE (continued)

$V$ .....	Volume of a system or a compartment
$W(m,t)$ .....	Distribution of water drops
$W(y,\tau)$ .....	Dimensionless distribution of water drops
$x_m(t)$ .....	Number of particles of size $m$ from kinetic model
$\bar{x}_m$ .....	Stochastic mean number of particles of size $m$

### Greek Symbols

$\alpha$ .....	Dimensionless group defined in Table 3.2
$\beta$ .....	Dimensionless group defined in Table 3.2
$\Upsilon_m(t)$ .....	Mass fraction of particles of size $m$ from kinetic model
$\langle \Upsilon_m(t) \rangle$ .....	Stochastic mean mass fraction of particles
$\Upsilon_n$ .....	$n$ th moment of ice distribution
$\nu$ .....	Dimensionless group defined in Table 3.2
$\mu_n$ .....	$n$ th moment of droplet distribution
$\rho$ .....	Density of vapor in the cloud
$\rho_a$ .....	Density of air in cloud
$\rho_h$ .....	Vapor density around an ice particle
$\rho_l$ .....	Density of liquid water

NOMENCLATURE ( continued )

- $\rho_w$  ..... Vapor density around a water droplet
- $\mathcal{P}(x_1, x_2, \dots, N_0/N)$  Conditional probability defined by  
eq. (2.22) variance
- $\psi(m/N)$  ..... Conditional probability defined by  
eq. (2.24)
- $\Psi$  ..... Dimensionless group defined in  
Table 3.2

Subscripts

- h ..... Ice particle
- H ..... Coagulation
- R ..... Riming
- w ..... Water droplet
- W ..... Coalescence

## CHAPTER 1

### INTRODUCTION

#### 1.1 PRELIMINARY REMARKS

Coalescence is the dominant mechanism for particle growth in various multiparticle systems such as aerosols and raindrops in the atmosphere. The collision mechanism, through which coalescence occurs, may vary from system to system. Examples of collision mechanisms are Brownian and turbulent motion in the case of aerosols, and differing terminal velocities in the case of raindrops in clouds. In such systems, knowledge of the particle size distribution in time is of great importance. A so-called "kinetic equation" has been formulated in the literature based on the assumption that the system always consists of a large population of randomly distributed particles which grow as a result of binary coalescence.

The basic discrete form of the kinetic equation is:

$$\frac{dx_m}{dt} = 1/2 \sum_{n=1}^{m-1} C_{n,m-n} x_n x_{m-n} - x_m \sum_n C_{mn} x_n \quad (1.1)$$

where  $x_m$  is the number of particles of  $m$  units mass in some volume. It is convenient to regard  $m$  also as an index of size and, accordingly,  $x_m$  is alternatively the number of particles of size  $m$  in the volume.  $C_{mn}$  is the collection coefficient and is a measure of the rate of coalescence for particles of sizes  $m$  and  $n$ . Additional terms are included

in eq. (1.1) when mechanisms other than coalescence affect the particle size distribution of a coalescing system.

## 1.2 AIM AND SCOPE OF THE THESIS

This thesis examines two separate but related problems in the area of multiparticle coalescing systems.

The first problem, which is investigated in Chapter 2, deals with the question of the validity of eq. (1.1), which neglects correlations. A stochastic model is set up and solved for the probabilities of all possible histories of particle growth. Results obtained from the stochastic model are used to study the effect of correlations in a coalescence process.

In Chapter 3, which comprises the second part of the thesis, kinetic equations of the form of eq. (1.1) are used to simulate the evolution of seeded supercooled stationary clouds.

Each chapter contains its own introduction and conclusions.

## CHAPTER 2

### THE EXTENT OF CORRELATIONS IN A STOCHASTIC COALESCENCE PROCESS

#### 2.1 INTRODUCTION

The evolution of many coalescing multiparticle systems has been examined through the use of kinetic equations of the form of eq. (1.1). For coalescence of raindrops in a cloud, the first analytic solution of eq. (1.1) was obtained by Golovin (1963) for a coalescence coefficient proportional to the sum-of-the-masses of the drops,  $C_{mn} = \text{constant} * (m+n)$ , where the initial distribution was exponential. This coalescence coefficient is a good approximation when the radii exceed  $25\mu$ . Scott (1967) obtained analytical solutions of eq. (1.1) for three different coalescence coefficients and two different initial distributions. He solved the equation for  $C_{mn} = \text{constant}$ ,  $C_{mn} = \text{constant} * mn$ , and  $C_{mn} = \text{constant} * (m+n)$ . His initial distributions were a Gaussian distribution and a distribution consisting of two discrete sizes. Drake and Wright (1972) obtained solutions of the kinetic equation when the coalescence coefficient was a linear combination of the coefficients studied by Scott,  $C_{mn} = A_1 + A_2 (m+n) + A_3 mn$ .

Twomey (1964), Berry (1967) and Warshaw (1967) used experimentally determined coalescence coefficients to obtain numerical solutions of eq. (1.1) for a cloud of water drops coalescing under various conditions. Hidy (1965) obtained numerical solutions of the kinetic equation for coagulation of aerosols by Brownian motion while Huang, Kerker, and Matijevic (1970) solved the equation

numerically for coagulation due to turbulent motion. Long (1971) examined the computational errors arising in numerical solutions of eq. (1.1).

The validity of the kinetic equation as a model for droplet coalescence in a warm cloud has been questioned by Warshaw (1967, 1968) and Long (1971, 1972). They claim that the kinetic equation is "stochastically incomplete" since it describes only the average behavior of cloud droplets and not the deviation from it. Scott (1967, 1968, 1972), Berry (1967, 1968), Gillespie (1972) and Slinn and Gibbs (1971) defend the validity of eq. (1.1) claiming that it includes the probabilities of all possible histories of droplet growth.

In this chapter we address this question. We shall set up a stochastic coalescence model that can furnish the probabilities of all histories of particle growth, and we shall then show that this model reduces to the kinetic equations when particle correlations are omitted. What emerges from the kinetic equations are hence not necessarily the true averages of the underlying random processes. The magnitude of these discrepancies depends on the extent of the correlations. Correlations may be particularly significant in systems of small populations, in which case the properties of individual particles are not statistically independent, and the outcome from the kinetic equations will accordingly not match the true stochastic averages.

On the other hand, we would expect correlations to diminish in systems of large populations. In that case we would find that variances and covariances become small, distributions become

singular, and the processes involved become essentially deterministic.

The question arises as to just how large a population ought to be before we are satisfied that kinetic equations describe its behavior satisfactorily. The answer to this question can be sought only in the complete formulation of the stochastic model from which the appropriate variances can be computed, and one can deduce the circumstances under which the standard deviation becomes a negligible fraction of the mean.

The trouble is that whenever we confront a system in which particles are correlated, the mathematics of the stochastic machinery becomes very formidable and even partial information is hard to obtain. We are fortunate in that the example we have picked for study in this chapter, namely particle growth by coalescence, has afforded us with the only system of significance we are aware of, in which we are able to obtain the full history of probability distributions. We hasten to note that in the interest of pushing the stochastic apparatus to the very end, we had to settle for the simplified case in which coalescence is characterized by a constant collection coefficient. We are aware of the shortcomings introduced by use of a constant collection coefficient, but we may note that the results obtained are, nonetheless, illuminating; moreover, in many dispersed-phase coalescing processes it has been established that a constant coefficient is appropriate, at least as a first approximation (Kapur and Fuerstenau, 1969; Knutson et. al., 1967).

Before closing these introductory remarks, we think it

appropriate to call attention to a recent paper by Gillespie (1972) that also deals with the stochastic modeling of the coalescence process. We find Gillespie's discussion thorough and lucid. He sets up the stochastic model for any general collection coefficient, but his solutions omit particle correlations. Two other noteworthy papers to which this study is complementary are those of Knight (1971) and Marcus (1968). Finally, a general discussion of probability methods in particulate systems is offered in a paper by (Katz and Shinnar, 1969).

## 2.2 FORMULATION OF THE STOCHASTIC MODEL

Specifying the state of the system at any time by the number  $N$  of particles present together with the numbers  $x_1, x_2, x_3$ , etc. of particles of sizes 1, 2, 3, etc., we describe the random mechanism of the process as follows: In a short time  $\Delta t$ , any two particles can coalesce with probability  $C \Delta t$ , where  $C$  is the constant coalescence coefficient.

Now, suppose that at time  $t + \Delta t$  we have the distribution  $N, x_1, x_2, \dots, x_N$ , and we let  $\Delta t$  be chosen sufficiently small so that during the time interval  $(t, t + \Delta t)$  there could be, in the entire system, at most one coalescence. Now we pose the following question: From what states could this distribution evolve in the transition time  $\Delta t$ ? A little reflection will show that there are basically three different ways in which the system can assume this distribution: 1) a coalescence takes place between two particles of the same size; 2) a coalescence occurs between two particles of different sizes; and 3) no coalescence occurs.

Let us consider each of these routes separately. If the system is to reach the desired distribution through a coalescence between two particles of the same size, it must be, at time  $t$ , at the state

$$N+1, x_1, \dots, x_m+2, \dots, x_{2m}-1, \dots, x_N.$$

The probability associated with this distribution is  $v(N+1, x_1, x_2, \dots, x_m+2, \dots, x_{2m}-1, \dots; t)$ , and the probability that two particles of size  $m$  will coalesce in the interval  $(t, t + \Delta t)$  is

$$\binom{x_m+2}{2} c \Delta t.$$

Accordingly, the system will change from state  $N+1, x_1, \dots, x_m+2, \dots, x_{2m}-1, \dots, x_N$  to the desired state in  $\Delta t$  with probability

$$\sum_m v(N+1, x_1, x_2, \dots, x_m+2, \dots, x_{2m}-1, \dots; t)$$

$$\times \binom{x_m+2}{2} c \Delta t.$$

If the system is to reach the desired distribution through a coalescence between two particles of different sizes, it must, at time  $t$ , be at the state

$$N+1, x_1, \dots, x_m+1, \dots, x_n+1, \dots, x_{m+n}-1, \dots, x_N.$$

The probability associated with this distribution at time  $t$  is  $v(N+1, x_1, x_2, \dots, x_m+1, \dots, x_{m+n}-1, \dots; t)$ , and the probability that two particles of sizes  $m$

and  $n$  will coalesce in the time interval  $(t, t+\Delta t)$  is  $(x_m+1)(x_n+1)C\Delta t$ . Hence, the system will change from state  $N+1, x_1, \dots, x_m+1, \dots, x_n+1, \dots, x_{m+n}-1, \dots, x_N$  to the desired state in the transition time  $\Delta t$  with probability

$$\sum_{m < n} \sum v(N+1, x_1, x_2, \dots, x_m+1, \dots, x_n+1, \dots, x_{m+n}-1, \dots; t) (x_m+1)(x_n+1)C\Delta t.$$

Finally, the probability of having the desired distribution at time  $t$  and no coalescence in the interval  $(t, t+\Delta t)$  is

$$v(N, x_1, x_2, \dots; t) \left[ 1 - \binom{N}{2} C \Delta t \right].$$

The probability  $v(N, x_1, x_2, \dots; t+\Delta t)$ , of having the desired distribution at time  $t+\Delta t$ , can now be expressed as the sum of the three mutually exclusive probabilities assembled above:

$$\begin{aligned}
& v(N, x_1, x_2, \dots; t + \Delta t) \\
&= \sum_m v(N+1, x_1, x_2, \dots, x_m+2, \dots, \\
&\quad x_{2m-1}, \dots; t) \binom{x_m+2}{2} C \Delta t \\
&+ \sum_{m < n} \sum v(N+1, x_1, x_2, \dots, x_m+1, \dots, x_n+1, \dots, \\
&\quad x_{m+n-1}, \dots; t) (x_m+1) (x_n+1) C \Delta t \\
&\quad + v(N, x_1, x_2, \dots; t) \left[ 1 - \binom{N}{2} C \Delta t \right]. \quad (2.1)
\end{aligned}$$

Now, bringing the term  $v(N, x_1, x_2, \dots; t)$  from right to left, dividing by  $\Delta t$  and letting  $\Delta t \rightarrow 0$ , one obtains

$$\begin{aligned}
& \frac{dv}{dt} (N, x_1, x, \dots; t) \\
&= C \sum_{m < n} \sum v(N+1, x_1, x_2, \dots, x_m+1, \dots, \\
&\quad x_n+1, \dots, x_{m+n-1}, \dots; t) (x_m+1) (x_n+1) \\
&+ C \sum_m v(N+1, x_1, x_2, \dots, x_m+2, \dots, \\
&\quad x_{2m-1}, \dots; t) \binom{x_m+2}{2} \\
&\quad - C v(N, x_1, x_2, \dots; t) \binom{N}{2}. \quad (2.2)
\end{aligned}$$

Eq. (2.2) is the fundamental expression of the stochastic description. Solution of eq. (2.2) will produce the complete probabilistic picture of the process, but, short of a complete solution, eq. (2.2) can also yield useful partial information in the form of suitable averages of the underlying random processes—means, variances, covariances, etc.

Before we present the solutions to eq. (2.2), we first proceed to demonstrate the circumstances under which (2.2) reduces to the kinetic equations.

### 2.3 THE KINETIC EQUATIONS

Let  $P(n,m;t)$  be the single-particle distribution associated with particles of size  $m$ ; that is,  $P(n,m;t)$  is the probability of finding  $n$  particles of size  $m$  at time  $t$ . And let  $\langle x_m(t) \rangle$  be the mean value of  $P(n,m;t)$ .  $P(n,m;t)$  can be obtained from  $v(N,x_1,x_2,\dots;t)$  by

$$P(n,m;t)$$

$$= \sum_N \sum_{x_1} \sum_{x_2} \cdots \sum_{\text{except } x_m} v(N,x_1,x_2,\dots,x_m=n,\dots;t), \quad (2.3)$$

$$\langle x_m(t) \rangle = \sum_n n P(n,m;t). \quad (2.4)$$

Accordingly, the differential equations governing  $x_m$  are:

$$\frac{d\langle x_m \rangle}{dt} = 1/2 C \sum \langle x_n, x_{n-1} \rangle - C \langle x_m^N \rangle + C \langle x_m \rangle, \quad m \text{ odd}, \quad (2.5a)$$

$$\begin{aligned} \frac{d\langle x_m \rangle}{dt} = 1/2 C \sum \langle x_n x_{m-n} \rangle - C \langle x_m^N \rangle + C \langle x_m \rangle \\ - 1/2 C \langle x_{m/2} \rangle, \quad m \text{ even}. \end{aligned} \quad (2.5b)$$

Making use of the identity

$$\text{Cov}(X, Y) = \langle XY \rangle - \langle X \rangle \langle Y \rangle,$$

where  $\text{Cov}(X, Y)$  denotes the covariance of the random variables  $X$  and  $Y$ , we may cast eqs. (2.5) in the form

$$\begin{aligned} \frac{d\langle x_m \rangle}{dt} = 1/2 C \sum & [\text{Cov}(x_n, x_{m-n}) + \langle x_n \rangle \langle x_{m-n} \rangle \\ & - C [\text{Cov}(x_m, N) + \langle x_m \rangle \langle N \rangle] \\ & + C \langle x_m \rangle, \quad m \text{ odd}, \end{aligned} \quad (2.6a)$$

$$\begin{aligned} \frac{d\langle x_m \rangle}{dt} = 1/2 C \sum & [\text{Cov}(x_n, x_{m-n}) + \langle x_n \rangle \langle x_{m-n} \rangle \\ & - C [\text{Cov}(x_m, N) + \langle x_m \rangle \langle N \rangle] \\ & + C \langle x_m \rangle - 1/2 C \langle x_{m/2} \rangle, \quad m \text{ even}. \end{aligned} \quad (2.6b)$$

Now, if in eqs. (2.6) we omit all covariances, we then obtain the kinetic equations. For the purpose of telling them apart, we produce the kinetic equations below without use of the angular brackets:

$$\frac{dx_m}{dt} = 1/2 C \sum_{n=1}^{m-1} x_n x_{m-n} - Cx_m(N-1), \quad m \text{ odd}, \quad (2.7a)$$

$$\frac{dx_m}{dt} = 1/2 C \sum_{n=1}^{m-1} x_n x_{m-n} - 1/2 Cx_{m/2} - Cx_m(N-1), \quad m \text{ even}. \quad (2.7b)$$

In the literature, the rate of coalescence between equi-size particles,  $Cx_m(x_m-1)/2$ , is normally approximated by  $Cx_m^2/2$  and, accordingly, both (2.7a) and (2.7b) reduce to a single expression

$$\frac{dx_m}{dt} = 1/2 C \sum_{n=1}^{m-1} x_n x_{m-n} - Cx_m N, \quad (2.8)$$

which is of the form of eq. (1.1) with a constant coalescence coefficient.

It is, of course, obvious that so long as the covariances remain appreciable, the results of the kinetic equations will not match the true stochastic averages from (2.5) or (2.6). On the other hand, in a particulate

system of sufficiently large "well mixed" population, covariances may become small, and comparison of eqs. (2.5) and (2.6) shows that the mean values  $\langle x_m N \rangle$  and  $\langle x_n x_{m-n} \rangle$  become approximately equal to the products  $\langle x_n \rangle \langle N \rangle$  and  $\langle x_n \rangle \langle x_{m-n} \rangle$ : that is, the distributions become singular and we may identify the  $x_m$  of the kinetic equations with the true mean values. Under these circumstances, the kinetic equations give an essentially complete description of the coalescence process. Just how large does the population have to be before these circumstances materialize? To answer this question we turn to the solutions of the stochastic equations. In the next two sections, we shall first obtain solutions dealing with the total number of particles, size notwithstanding, and then proceed to deduce the solutions for the size spectrum. In each case comparisons will be drawn to the corresponding results from the kinetic equations.

## 2.4 SOLUTIONS I: THE TOTAL NUMBER OF PARTICLES

In terms of  $v(N, x_1, x_2, \dots; t)$ , the probability  $v_N(t)$  of having  $N$  particles of whatever size at any moment is

$$v_N(t) = \sum \sum \dots \sum \sum_{\text{sum over all } x_m \text{'s}} v(N, x_1, x_2, \dots; t) \quad (2.9)$$

And from eq. (2.2) we deduce

$$\frac{dv_N}{dt} = c \binom{N+1}{2} v_{N+1} - c \binom{N}{2} v_N. \quad (2.10)$$

For a uniform initial distribution comprising  $N_0$  particles of size unity

$$v_N(0) = \delta_{N, N_0}, \quad (2.11)$$

and in Appendix A we show that eq. (2.10) admits the solution

$$v_N(t) = \sum_{k=n}^{N_0} \frac{(-1)^{k+N} (2k-1) (k+N-2)!}{N! (N-1)! (k-N)!} \times \prod_{\nu=0}^{k-1} \left( \frac{N_0 - \nu}{N_0 + \nu} \right) \exp \left[ -c \binom{k}{2} t \right]. \quad (2.12)$$

The mean number of particles,  $\langle N \rangle$ , at any time comes to

$$\langle N \rangle = \sum_{k=N}^{N_0} NV_N = \sum_{k=N}^{N_0} (2k-1) \times \prod_{\nu=0}^{k-1} \left( \frac{N_0 - \nu}{N_0 + \nu} \right) \exp \left[ -C \binom{k}{2} t \right]. \quad (2.13)$$

The corresponding results from the kinetic equations are obtained as follows: Summing (2.7a) and (2.7b) over all  $m$ 's yields

$$\frac{dN}{dt} = -\frac{1}{2}CN(N-1), \quad (2.14)$$

which, subject to the initial condition  $N(0)=N_0$ , produces the solution

$$N = \frac{N_0}{N_0 - (N_0 - 1) \exp(-\frac{1}{2}ct)} \quad (2.15)$$

Before we proceed to illustrate the above solutions numerically, it may perhaps be instructive to compare

eq. (2.14) and the differential equation that governs the true mean number of particles; the latter is obtained by multiplying (2.10) by  $N$  and summing over  $N$ :

$$\frac{d\langle N \rangle}{dt} = -\frac{1}{2}C \sum N(N-1) v_N = -\frac{1}{2}C [ \langle N^2 \rangle - \langle N \rangle ]. \quad (2.16)$$

The kinetic equation obviously differs from the equation for the true mean. Indeed, we may write the latter as

$$\frac{d\langle N \rangle}{dt} = -\frac{1}{2}C [ \langle N \rangle^2 - \langle N \rangle + \sigma^2 ], \quad (2.17)$$

where  $\sigma^2 = \langle N^2 \rangle - \langle N \rangle^2$  is the variance, and conclude that as long as  $\sigma^2 \neq 0$ , the number of particles,  $N$ , obtained from the kinetic equations will exceed the true mean  $\langle N \rangle$  at any given moment, and will coincide with it only when the variance  $\sigma^2$  becomes a small fraction of the mean. The exact measure of these differences will presently be sought in the numerical solutions.

Turning now to some numerical examples, we note first that, even for small values of  $N_0$ , eqs. (2.13) and (2.15) can hardly be told apart: see, for example, the solutions for  $N_0=10$  and  $N_0=20$  shown in Fig. 2.1. In Fig. 2.2 we have plotted the variance

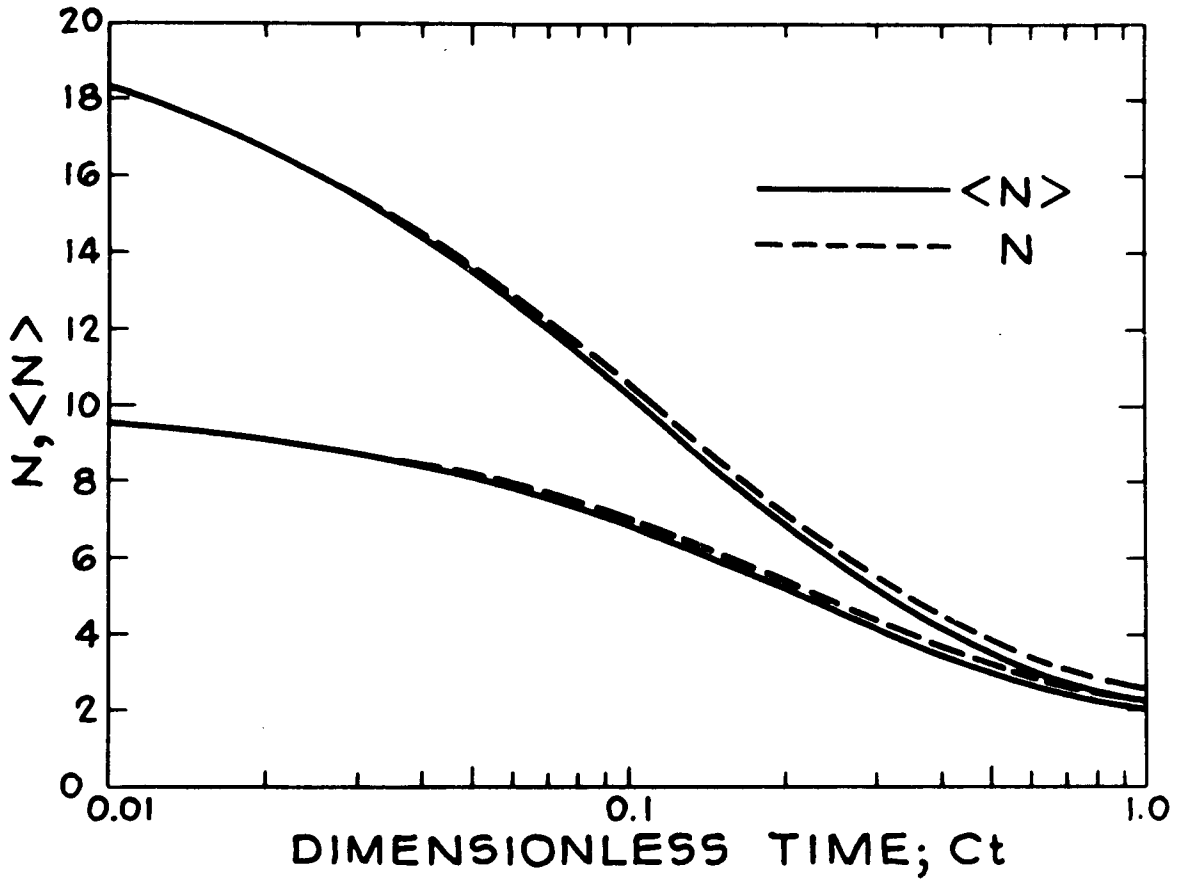


Fig. 2.1  $\langle N \rangle$  and  $N$  as functions of  $Ct$ .  $\langle N \rangle$  is given by eq. (2.35) and  $N$  by eq. (2.36)

$\sigma^2$  and the mean  $\langle N \rangle$ , as functions of  $Ct$  for the case in which  $N=20$ . Accordingly, just as we have noted above, the variance is indeed, for the most part, small compared to the mean; it stands to reason that for larger values of  $N_0$ , the variance will become a vanishingly small fraction of the mean, and the distribution will become practically singular. This is not in agreement with the results of Scott (1967; Section 6) who claimed that  $v_N(t)$  obeys Poisson statistics. We hasten, however, to note that, in reference to eq. (2.17), when  $N_0$  is large the term  $\langle N \rangle^2$  dominates and it makes little practical difference whether the distribution is Poisson ( $\sigma^2 - \langle N \rangle = 0$ ), or whether, as is indeed the case, the distribution is singular ( $\sigma^2 / \langle N \rangle \rightarrow 0$ ).

As a matter of fact, even when the initial distribution is Poisson, rather than the uniform distribution of eq. (2.11), we find that the evolution of the particle count does not follow Poisson statistics. For an initial Poisson distribution whose mean is  $\langle N_0 \rangle$ , we have

$$v_N(0) = \frac{\exp(-N_0) \langle N_0 \rangle^N}{N!} \quad (2.18)$$

and eq. (2.10) now yields

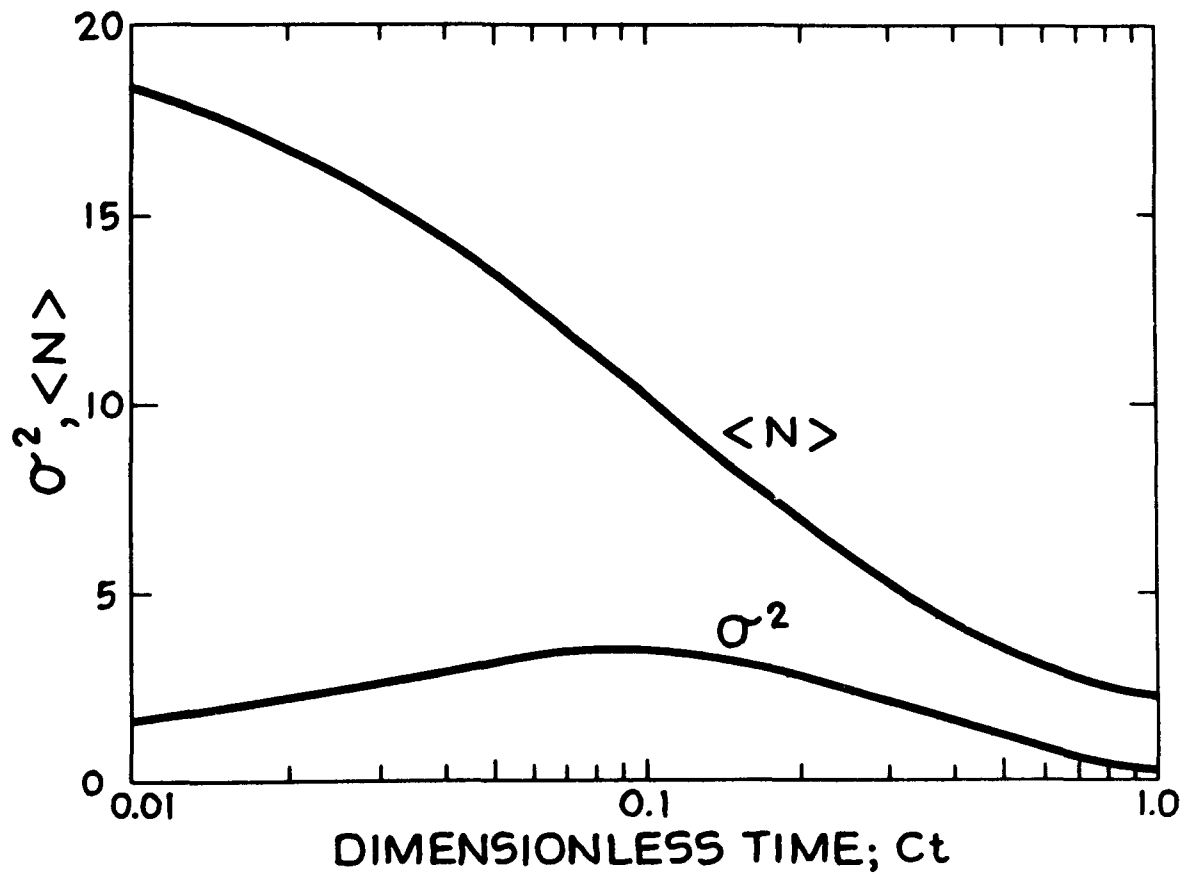


FIG. 2.2. The variance,  $\sigma^2$ , and the mean,  $\langle N \rangle$ , as functions of  $Ct$ .  
 $N_0 = 20$ .

$v_N(t)$ 

$$\begin{aligned}
 & N_{0,\max} N_{0,\max} e^{-\langle N_0 \rangle} \langle N_0 \rangle^{\ell} (-1)^{k+N} (2k-1) (k+N-2)! \\
 = & \sum_{k=N} \sum_{\ell=k+1} \frac{\quad}{\ell! N! (N-1)! (k-N)!} \\
 & \times \prod_{\nu=1}^{k-1} \left( \frac{\ell-\nu}{\ell+\nu} \right) \exp \left[ -c \binom{k}{2} t \right] \quad (2.19)
 \end{aligned}$$

where  $N_{0,\max}$  is the largest value of  $N_0$  which has a significant probability in the initial distribution. The mean number  $\langle N \rangle$  of particles for a Poisson initial distribution accordingly becomes

$$\begin{aligned}
 \langle N(t) \rangle = & \sum_{k=1}^{N_{0,\max}} \sum_{\ell=k+1}^{N_{0,\max}} \frac{e^{-\langle N_0 \rangle} \langle N_0 \rangle^{\ell} (2k-1)}{\ell!} \\
 & \times \prod_{\nu=1}^{k-1} \left( \frac{\ell-\nu}{\ell+\nu} \right) \exp \left[ -c \binom{k}{2} t \right], \quad (2.20)
 \end{aligned}$$

In Fig. 2.3 we have plotted  $\sigma^2 / \langle N \rangle$  as a function of  $Ct$

for a Poisson initial distribution with 20 particles as its mean; and in Fig. 2.4a we have compared the histogram distribution  $v_N(t)$  at a point in time when the mean has reached 8.9 with a Poisson distribution of the same mean; Fig. (2.4b) is a continuous version of Fig. (2.4a). We may note here that throughout the remainder of this chapter we have found it more convenient, for illustrative purposes, to use continuous curves in place of histograms.

Before we leave this particular subject matter, we wish also to note that, at any moment, the mean number of particles that evolve from a uniform initial distribution and from a Poisson initial distribution are virtually the same: Witness Fig. 2.5 in which we have compared these means, as functions of  $Ct$ , for  $\langle N_0 \rangle = 20$ .

The results of this section can be summarized briefly as follows: Insofar as the mean number of particles is concerned, disregarding size distribution, the results of the kinetic and the full stochastic equations are nearly indistinguishable even when initial populations are quite small. We have to admit, however, that it is likely that this result will change considerably if the coalescence coefficient be made to depend on particle size. It stands to reason that in such a case particle correlations would be stronger than in a system governed by a constant collection coefficient.

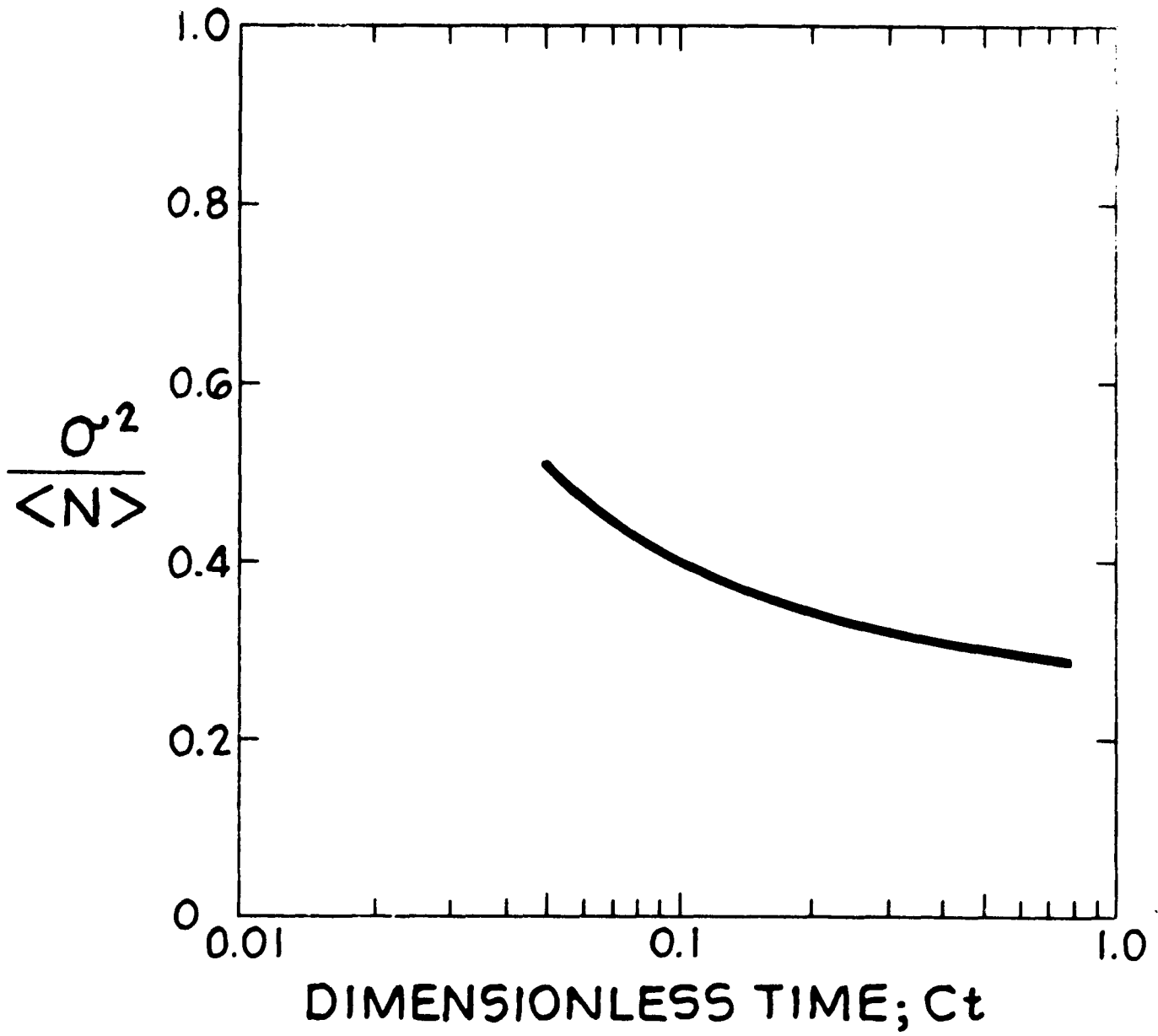


Fig. 4.3.  $\sigma^2 / \langle N \rangle$  for a Poisson initial distribution with  $\langle N_0 \rangle = 20$ .

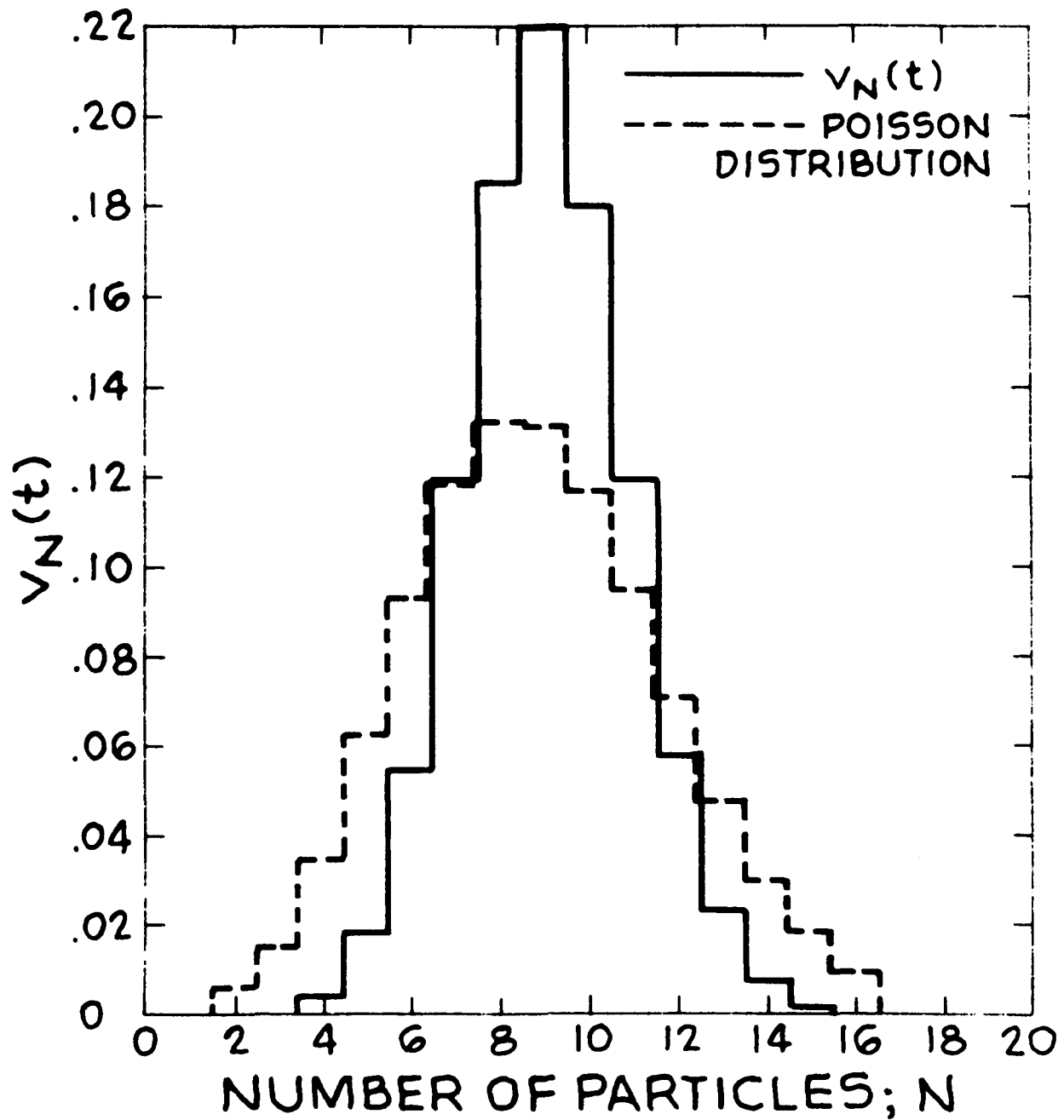


Fig. 2.4a.  $v_N(t)$  when  $\langle N \rangle = 8.9$  ( $\langle N_0 \rangle = 20$ ,  $Ct = 0.125$ ) compared to the Poisson distribution with the same mean.

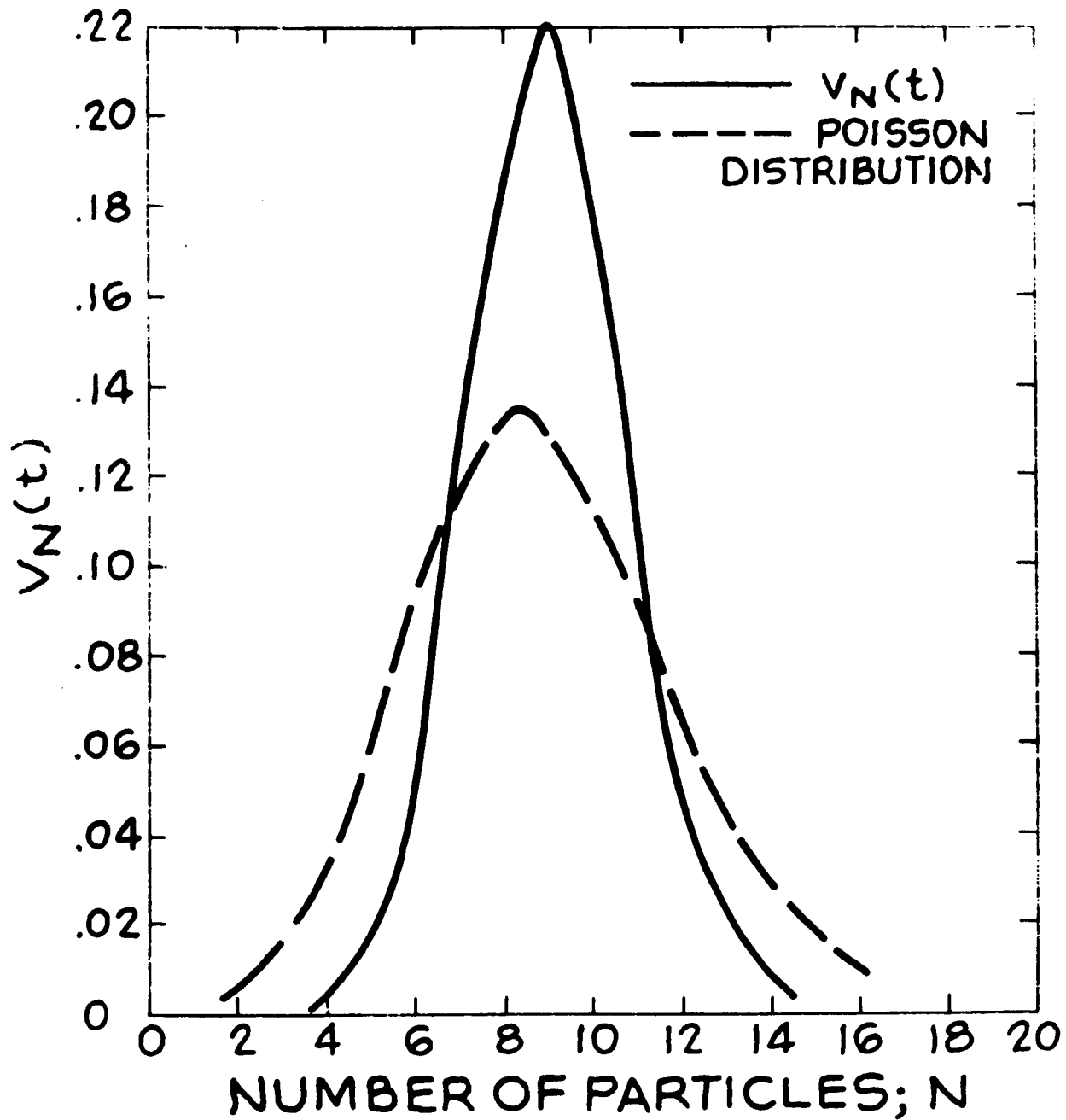


Fig. 2.4b. .  $v_N(t)$  when  $\langle N \rangle = 8.9$  ( $\langle N_0 \rangle = 20$ ,  $Ct = 0.125$ ) compared to the Poisson distribution with the same mean. (Continuous version of Fig. 2.4a.)

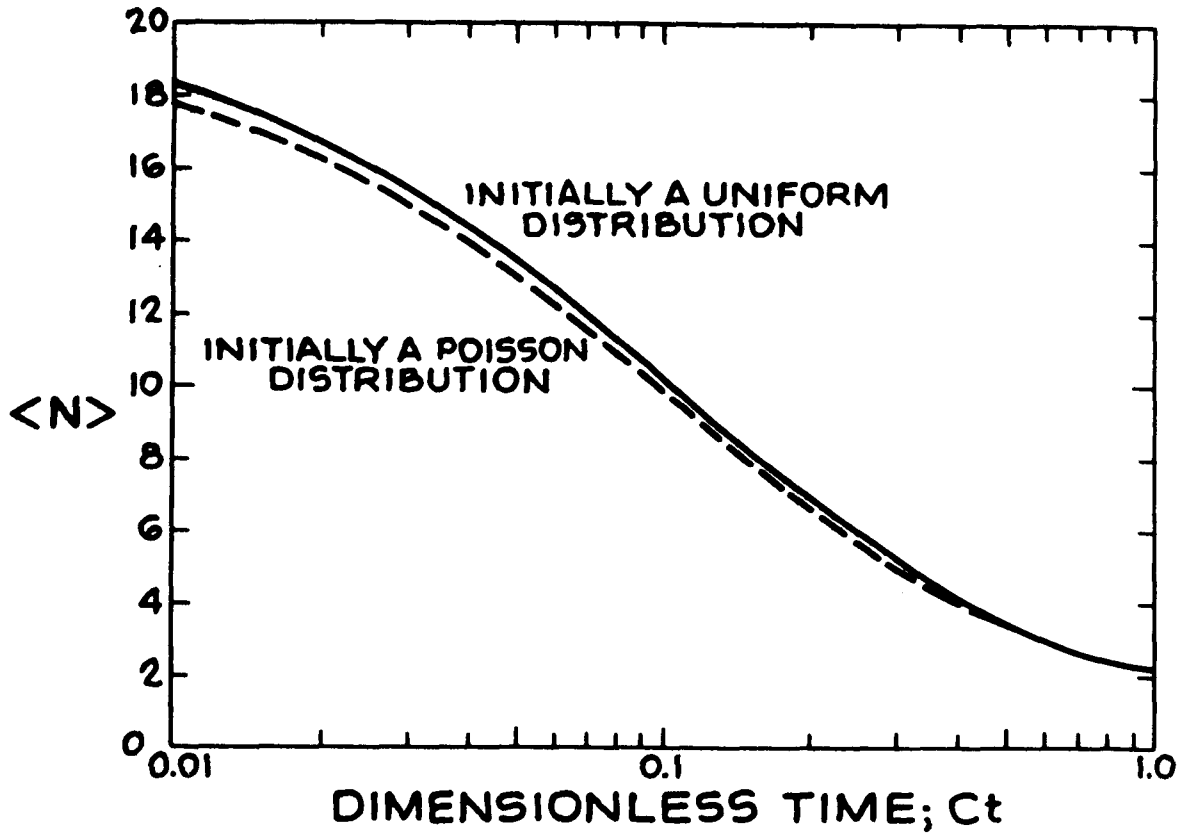


Fig. 2.5. The mean number of particles arising from a uniform initial distribution and from a Poisson initial distribution;  $\langle N_0 \rangle = 20$ .

## 2.5 SOLUTIONS II: THE SIZE SPECTRUM

Eq. (2.2) may seem quite formidable. As it turns out, for an initial population of  $N_0$  particles of unit size, a relatively simple solution emerges:

$$v(N, x_1, x_2, \dots; t) = Q(x_1, x_2, \dots, x_{N_0}/N) v_N(t), \quad (2.21)$$

where  $v_N(t)$ , on which the previous section was focused, is the probability of having  $N$  particles of any size, and the time-independent  $Q(x_1, x_2, \dots, x_{N_0}/N)$  is the probability of having a specified size distribution given that there are  $N$  particles. The function  $Q$  is given by

$$Q(x_1, x_2, \dots, x_{N_0}/N) = \frac{\binom{N}{x_1} \binom{N-x_1}{x_2} \dots \binom{N-x_1-x_2-\dots-x_{N_0-1}}{x_{N_0}}}{\binom{N_0-1}{N-1}} \quad (2.22)$$

In the above, the numerator gives the number of ways in which a specific distribution of  $N_0$  units of mass in  $N$  particles can be obtained, and the denominator represents the total number of ways of distributing  $N_0$

units of mass in  $N$  particles (Feller, 1966; pp. 38-44).

We offer no formal proof that eq. (2.21) is the solution of (2.2). Instead, we have shown (see Appendix B) that  $(Q v_N$  does indeed satisfy the differential equation (2.2) and in a few highly simplified cases we were able to grind out numerical solutions that establish eq. (2.21) as the solution to (2.2).

With  $v(N, x_1, x_2, \dots; t) = (Q v_N$  at hand we may proceed to determine the single particle distributions  $P(n, m; t)$  and their mean values  $\langle x_m(t) \rangle$ .

There has been a great deal of discussion as to whether or not the  $P(n, m; t)$  obey Poisson statistics. Accordingly, in Fig. 2.6 and 2.7, we have generated the distributions  $P(n, 2; t)$  and  $P(n, 5; t)$  for  $N_0=20$ , each at three successive times and, for comparison, we have added the Poisson distributions that correspond to the respective mean values of  $P(n, 2; t)$  and  $P(n, 5; t)$ . The trend that emerges in Figs. 2.6 and 2.7 indicates that as time increases  $P(n, m; t)$  approaches a Poisson distribution. Gillespie (1972) showed this to be also true for a variable collection coefficient in the absence of correlations.

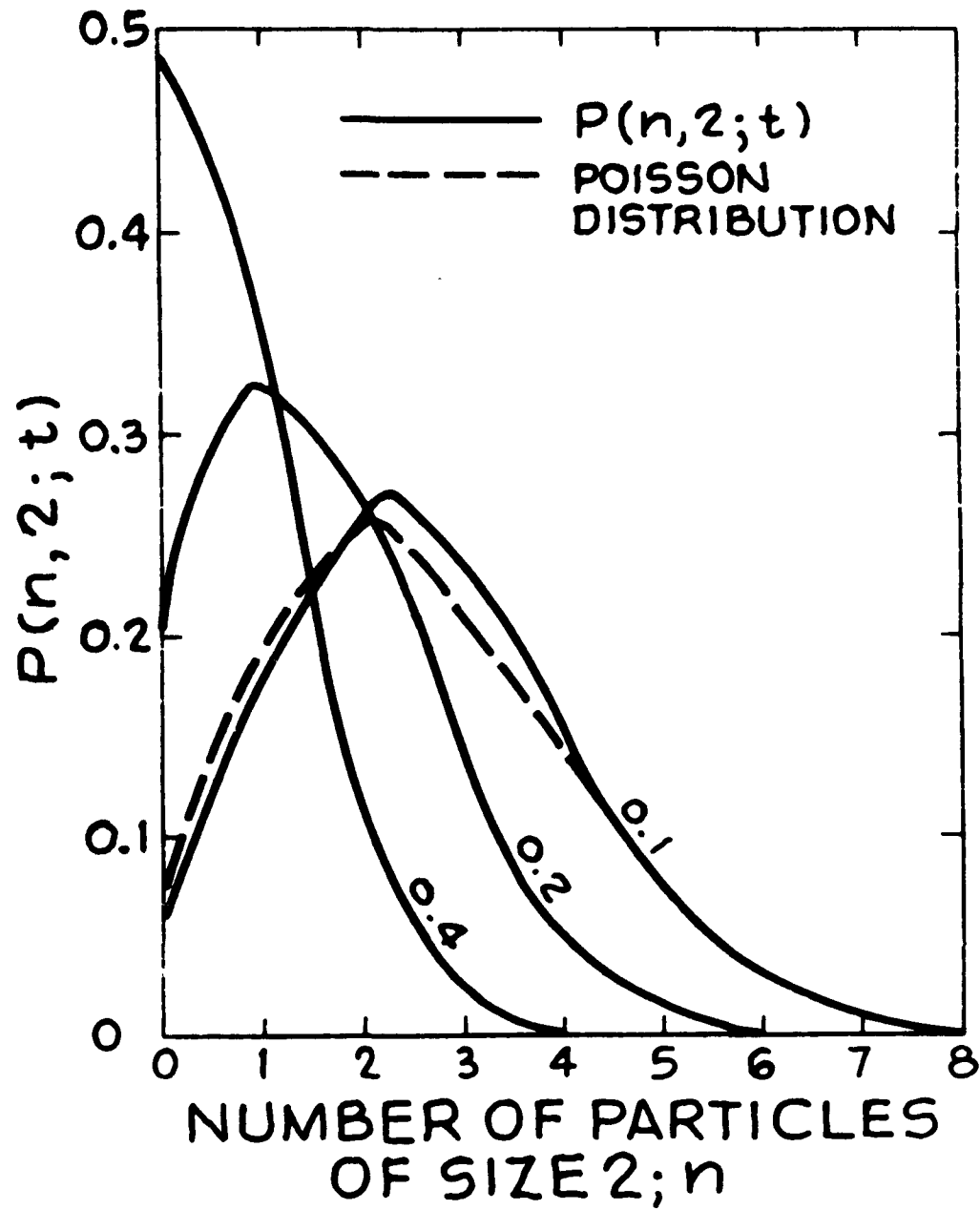


Fig. 2.6.  $P(n, 2; t)$  and Poisson distribution with the same mean at three successive values of  $Ct$ .  $N_0 = 20$ .

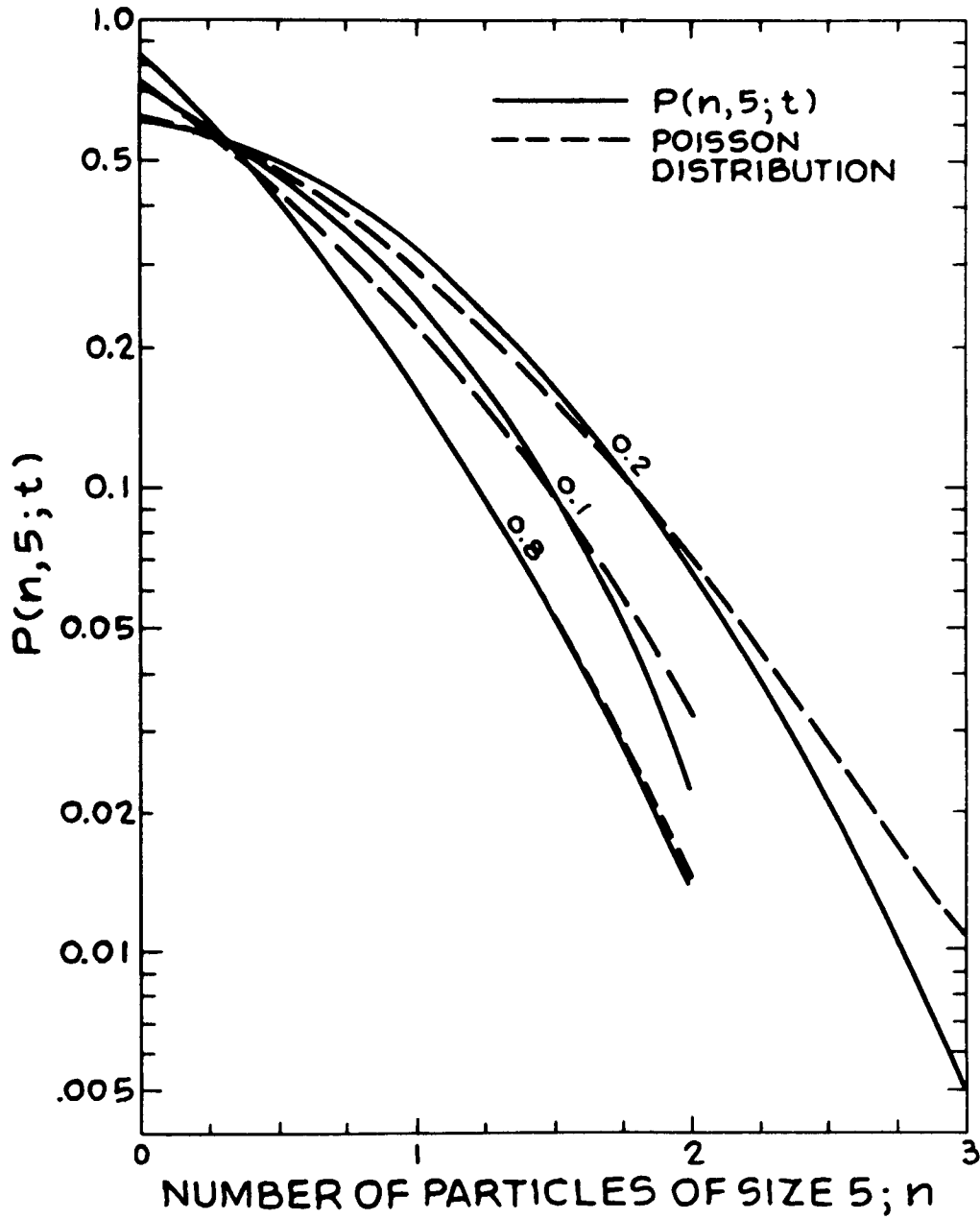


Fig. 2.7.  $P(n, 5; t)$  and Poisson distribution with the same mean at three successive values of  $Ct$ .  $N_0 = 20$ .

## 2.6 CORRELATIONS IN POORLY-MIXED SYSTEMS

So far our remarks have applied to any dispersed system of coalescing particles. We wish now to address specifically the subject of droplet growth in a warm cloud in order to illustrate an important consideration.

A real cloud is obviously a system of an enormously large population. On that account, one may argue that particle correlations in a cloud ought to be vanishingly small, and one may accordingly use the kinetic equation to model the growth of the droplets. The kinetic equation, however, is predicated on the assumption that the droplets are randomly distributed in the cloud—the so-called "well-mixed cloud" assumption. This is not normally the case in a real cloud: real clouds are not well-mixed. Hence, as droplets in a given region undergo a series of coalescences, there is a corresponding decrease in the number of droplets in that region available for further coalescence. Also, in a well-mixed cloud, it is possible to conceive the formation of very large particles in short times; in the real cloud there is some limit on the size a droplet may attain because of the finite amount of mass contained in the droplets in its immediate vicinity.

This is precisely the type of situation that brings about particle interactions or correlations. It is a situation that is rather difficult to model

mathematically, and, accordingly, in order to get some feeling on this matter, we have resorted to a simple device: We consider a large hypothetical cloud, which for all practical purposes may be regarded as infinitely large, partitioned into many small compartments of volume  $V$  with the understanding that droplets can coalesce only if they inhabit the same compartment. By making the compartment sufficiently small, we introduce particle interactions that are suggestive of the "local" interactions in a real cloud.

We shall describe the growth of particles within each compartment by the kinetic equations and by the full stochastic equations and compare the results. Accordingly, from eqs. (2.13) and (2.15), with  $C$  replaced by  $C=K/V$ , we may deduce, respectively, the mean (stochastic) particle concentration,  $\langle f \rangle = \langle N \rangle / V$ , in the total system, and its kinetic counterpart,  $f = N/V$ . In Fig. 2.8 we have drawn these two concentrations as functions of  $Kt$ , for the case in which  $f_0 = 100$  and, in turn,  $N_0 = 100, 50$  and  $10$ .

tion  $\langle f \rangle$  is  
 ... and that for  $N_0 = 100$ , the stochastic concentration  $\langle f \rangle$  is virtually identical to the kinetic concentration  $f$ ; when  $N_0$  equals  $10$  or  $50$ ,  $\langle f \rangle$  exceeds  $f$  slightly. Accordingly, for the choice of a constant collection coefficient, our results indicate that the number of particles per unit volume in the entire system at any

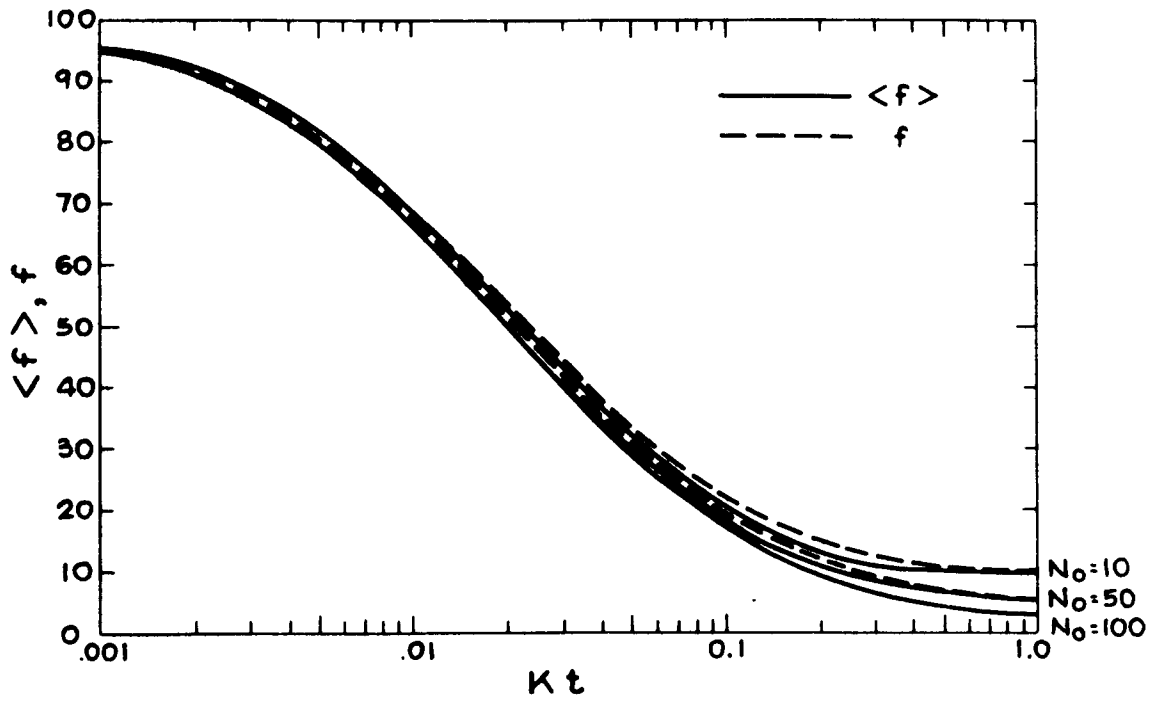


Fig 2. 8. Comparison between the stochastic concentration,  $\langle f \rangle$ , and the deterministic concentration,  $f$ , in a partitioned volume.  $f_0 = 100$ ;  $N_0 = 10, 50, 100$ .

time is insensitive to the type of poor mixing simulated by the partitioning model.

We next consider the important question of the evolution of the size distribution in the partitioned system. As the primary parameter, we focus upon the mean fraction  $\langle Y_m(t) \rangle$  of the total mass contained in particles of size  $m$ . With  $N_0$  being the total mass in each compartment, we have

$$\langle Y_m(t) \rangle = \frac{m \langle x_m(t) \rangle}{N_0} . \quad (2.23)$$

As a matter of computational convenience, we introduce the probability

$$\psi(m/N) = \frac{\binom{N-m-1}{N-2}}{\binom{N_0-1}{N-1}} , \quad m=1,2,\dots,N_0-N+1 \quad (2.24)$$

that a particle picked at random for a compartment containing  $N$  particles will be precisely of size  $m$ . With  $\psi(m/N)$  we have

$$\langle x_m(t) \rangle = \sum_N N v_N(t) \psi(m/N) , \quad (2.25)$$

and accordingly

$$\langle Y_m(t) \rangle = (m/N_0) \sum_N N v_N(t) \psi(m/N). \quad (2.26)$$

The corresponding mass fraction from the kinetic equation is  $Y_m(t)$ . We have solved the set of equations (2.7a) and (2.7b) numerically, and have also obtained a closed-form solution to (2.8). (The latter is the version that usually appears in the rain literature.) For initial populations as low as 10, the solutions to (2.7a) and (2.7b) on the one hand and to (2.8) on the other were indistinguishable. Hence, we record below the solution to eq. (2.8):

$$f(m,t) = x_m(t)/V = \frac{f_0 (\frac{1}{2}f_0 Kt)^{m-1}}{(1 + \frac{1}{2}f_0 Kt)^{m+1}}. \quad (2.27)$$

The kinetic mass fraction,  $Y_m(t)$ , then becomes

$$Y_m(t) = mf(m,t)/f_0 = \frac{m (\frac{1}{2}f_0 Kt)^{m-1}}{(1 + \frac{1}{2}f_0 Kt)^{m+1}}. \quad (2.28)$$

Figs. 2.9, 2.10, and 2.11 compare  $\langle Y_m(t) \rangle$  and  $Y_m(t)$  at three successive times;  $f_0$  was taken to be 100, and

values of  $N_0=10, 20, 50$  and  $100$  were used. These figures tell a significant story: for low values of  $N_0$  (i.e., in small compartments) there are substantial discrepancies between the size distributions obtained from the kinetic equation and the corresponding stochastic results, particularly in the long end of the distribution tail. The differences, however, diminish sharply as the compartments are chosen larger, and, more moderately, with time.

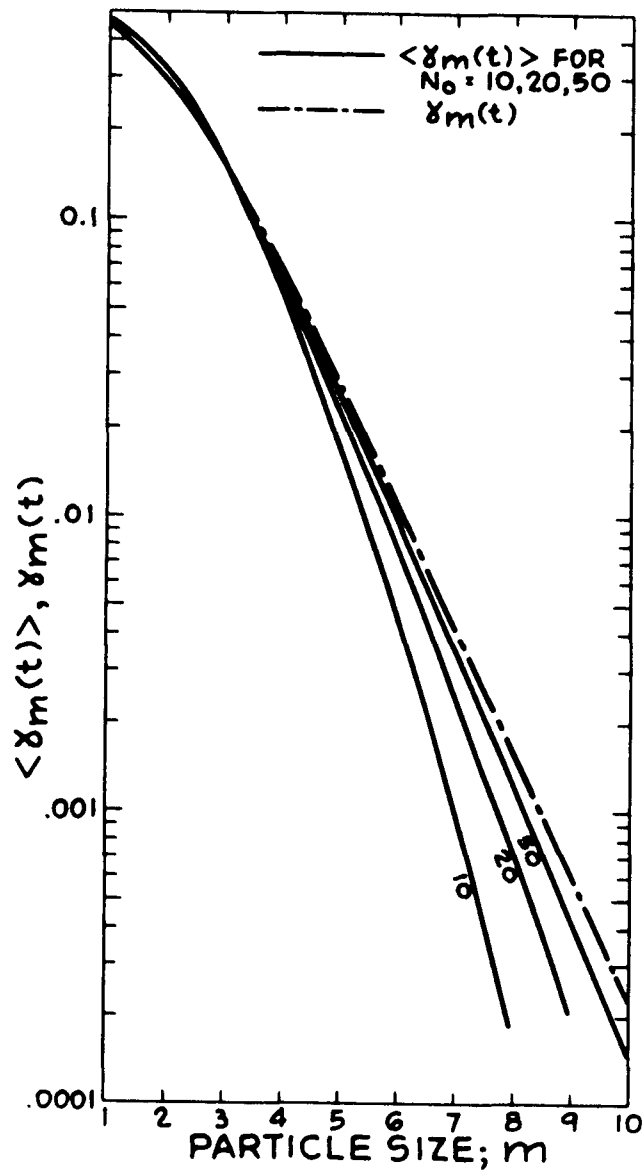


Fig. 2.9. Mass fraction distribution at  $Kt = .01$ .

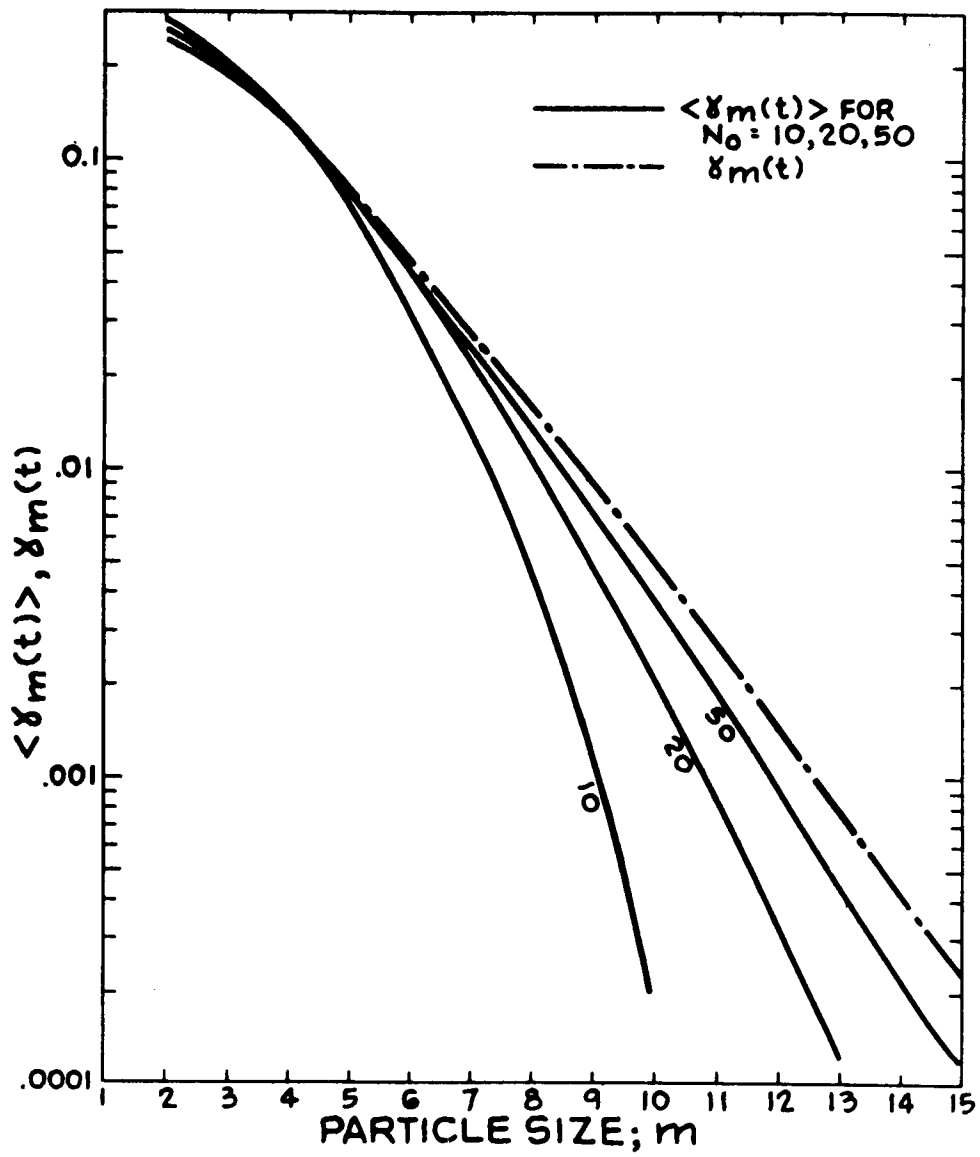


Fig. 2.10. Mass fraction distribution at  $Kt = .02$ .

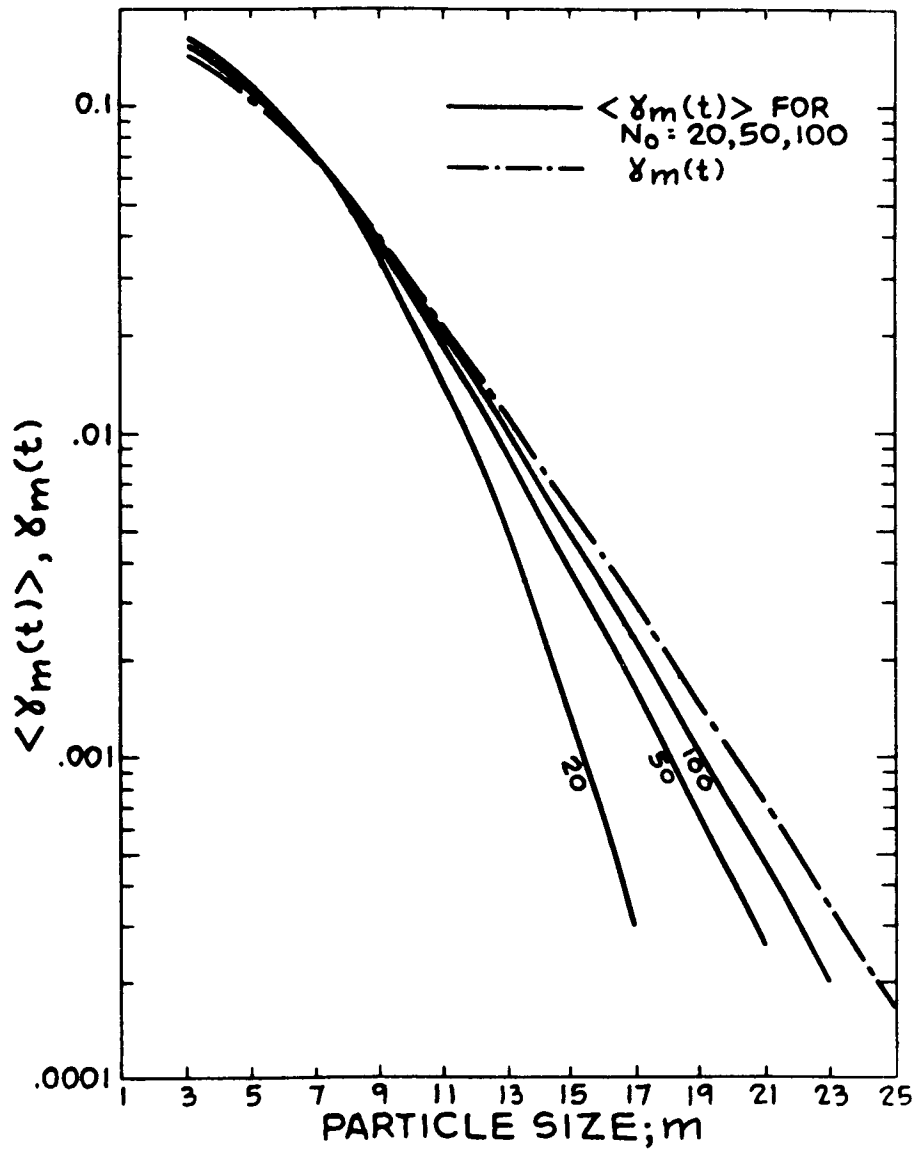


Fig. 2.11. Mass fraction distribution at  $Kt = .04$ .

## 2.7 CONCLUSIONS

Our aim in this chapter was to compare the kinetic and the full stochastic description of the growth of particles in a coalescing process. We discussed and illustrated the conceptual differences between these two approaches, and went on to examine their practical implications. We have argued that in well-mixed systems of large populations, the overall behavior of the particles is adequately described by the kinetic equations, but that in poorly mixed systems or in systems of small populations, statistical fluctuations become important and the outcome from the kinetic equations may differ appreciably from the true stochastic means. These discrepancies are caused by particle interactions or correlations. In systems of small population, for example, the probability, say, of having  $x_m$  particles of size  $m$ , is dependent on how many particles of various other sizes are also present.

We have set up and solved a stochastic model that can furnish the probabilities of all possible histories of particle growth. Our concession to our mathematical shortcomings was the choice of a constant coalescence coefficient; otherwise, our development is free of any further simplifying assumptions.

To study the consequences of poor mixing, we used a simple device: we partitioned the system into hypotheti-

cal, small, well-mixed compartments, and postulated that it was impossible for two particles of different compartments to coalesce.

Our results can be summarized briefly as follows: If we are merely interested in the total number of particles, regardless of their size distribution, then we find that for initial populations comprising as few as 10 particles, the results of the kinetic equation match the true stochastic averages. On the other hand, if we focus on the size distribution of the coalescing particles, we find that in systems of small population, or in a system partitioned into small compartments, the results of the kinetic equations may differ substantially from the stochastic means, particularly in the long-term tail of the distribution.

Before we draw lessons from these results, we should perhaps note our belief that if we were to solve the stochastic equations using a coalescence coefficient that depends on particle size, we would find the difference between the stochastic and the corresponding kinetic results amplified relative to the results with a constant collection coefficient.

Two lessons can be drawn from this study. First, if the behavior of few large particles govern some predominating phenomenon in a coalescing system, and if we have reason to believe that the system is poorly

mixed, then use of the kinetic model may produce significant errors. On the other hand, if the behavior of a coalescing system depends basically on the number of particles present in the system, regardless of their size spectrum, then the kinetic model can be used with a high degree of confidence.

The second problem has to do with the modeling of large systems that are well mixed. We expect correlations in such systems to be insignificant, but often, in order to model them, we employ numerical simulation methods, such as the Monte Carlo method, which use a relatively small population. This will introduce interactions, and computations in the tail will incur some errors.

## CHAPTER 3

### THE EFFECT OF SEEDING ON PARTICLE GROWTH IN SUPERCOOLED CLOUDS

#### 3.1 INTRODUCTION

It is generally accepted that the chance that a supercooled cloud would produce rain can be improved by increasing the concentration of ice particles in the cloud through seeding with silver iodide.

Two mechanisms have been proposed to explain how seeding may induce rain: Since ice has a lower vapor pressure than water, Bergeron (1935) postulated that diffusional growth of ice particles at the expense of water droplets would increase the chance of rain. This effect is believed to be particularly strong during the early development of the cloud when coalescence rates are small.

The second mechanism has been proposed by Simpson, et al. (1965). They claim that the release of latent heat of fusion during glaciation can significantly increase the cloud bouyancy and thereby invigorate the updraft, leading to a more rapid growth.

The precise mechanism notwithstanding, it is clear that seeding would increase the chance of rain to the extent that it can accelerate the overall growth of particles in the cloud. In this chapter we examine the effect of

seeding upon the growth of particles in a supercooled cloud. To this end, we have set up a mathematical model in which the cloud comprises four phases: ice particles, water drops, water vapor, and particles of silver iodide. With dynamic effects neglected, the model embodies six microphysical processes affecting the size distributions of the ice particles and the water drops. The six processes, grouped under three categories, are:

#### Collection Processes

- (1) Coalescence of water drops.
- (2) Coagulation of ice particles.
- (3) Riming of water drops on ice particles.

#### Diffusional Processes

- (4) Accretion of ice particles from the vapor phase.
- (5) Evaporation of water drops.

#### Ice Nucleation

- (6) Nucleation of ice particles produced from water drops by silver iodide.

The concentration of silver iodide in the cloud is clearly of considerable importance in determining the relative contributions of each of the above processes. In a heavily seeded cloud, coagulation of ice particles would provide the dominant growth mechanism, whereas growth in an unseeded cloud would be mostly by coales-

cence of water drops. The optimum seeding level corresponds to the seed concentration that would bring about maximum overall rate of growth of particles in the combined population of ice particles and water drops. We shall examine the optimum seeding level.

Of the six microphysical processes listed above, many have been examined separately, and there are several studies of a combination of up to four of these processes. But the combined effect of all six processes has not yet found expression in a single analysis.

Stalevich and Uchevatkina (1968) used a highly simplified continuous growth model to investigate the effect of seeding concentration on rain formation. They, however, assumed that during the lifetime of the cloud the variances of the distributions of both the ice particles and the water drops were zero. They also ignored the coagulation of ice particles. Ryan (1973) used integro-differential kinetic equations to model a cloud seeded with ice particles. His analysis ignores coalescence of water drops and coagulation of ice particles. Ryan found the optimum initial ice concentration to be about  $10^4 \text{m}^{-3}$ . Braham and Sievers (1955), using a highly simplified model, placed this concentration in the range  $10^5 - 10^6 \text{m}^{-3}$ .

Koenig (1966) also used a continuous growth model to examine the natural glaciation of a cloud for different initial ice concentrations. Unfortunately, he computed only the times necessary to reach given levels of glaciation, and deduced the evolution of the spectra for only one value of the initial ice concentration. Besides these studies, there have been investigations of the growth of individual ice particles in unseeded supercooled clouds. Some of the recent studies have been by Hindman and Johnson (1972), Marwitz and Auer (1968), and Takeda (1968).

Our model arises from mass balances on the inventories of solid, liquid and vapor in the cloud. It is in the form of integro-differential equations which describe the evolution of the distributions of ice particles and water drops. In the literature, these types of equations have often been labeled "stochastic"; we prefer to dub them "kinetic". These terms were thoroughly discussed in the previous chapter. The kinetic equations will be converted to equations in the moments of the distributions to which approximate solutions can be obtained. These solutions provide a better understanding of the evolutions of seeded clouds and the effect of various para-

meters on the six microphysical processes that contribute to that evolution.

### 3.2 FORMULATION OF THE MODEL

The model comprises two mass balances; one balance on the water and the other on the ice. We assume the cloud to be a closed (no inflow or outflow of mass), stationary, well-mixed, isothermal system. All particles are regarded as spherical, and no particle breakup or production is allowed. We shall also consider the density of the ice particles to be  $1 \text{ gm/cm}^3$ .

Let  $H(m,t)$  and  $W(m,t)$  be the number densities per unit volume of the ice particles and the water drops, respectively. That is,  $H(m,t)dm$  is the number of ice particles per unit volume whose size is in the range of  $m$  and  $m + dm$ , and  $W(m,t)dm$  is similarly defined for water.

The ice balance accordingly is:

$$\left(\frac{\partial H}{\partial t}\right) = \left(\frac{\partial H}{\partial t}\right)_{\text{coagulation}} + \left(\frac{\partial H}{\partial t}\right)_{\text{riming}} + \left(\frac{\partial H}{\partial t}\right)_{\text{accretion}} + \left(\frac{\partial H}{\partial t}\right)_{\text{nucleation}}. \quad (3.1)$$

and the water balance is:

$$\left(\frac{\partial W}{\partial t}\right) = \left(\frac{\partial W}{\partial t}\right)_{\text{coalescence}} + \left(\frac{\partial W}{\partial t}\right)_{\text{riming}} + \left(\frac{\partial W}{\partial t}\right)_{\text{evaporation}} + \left(\frac{\partial W}{\partial t}\right)_{\text{nucleation}}. \quad (3.2)$$

In the above equations,  $\partial H / \partial t$  is balanced against the changes in the spectra that result from the microphysical processes that affect the ice distribution, and  $\partial W / \partial t$  equals the changes in the spectra that result from the micro-

physical processes that affect the water drop distribution.

To formulate the exact expressions of all terms appearing on the right hand sides of eqs. (3.1) and (3.2), we now proceed to examine separately each of the six microphysical processes:

### Coalescence

The expression for the rate of change of the particle spectrum in a coalescing system is well known and often appears in the rain literature:

$$\left( \frac{\partial W(m, t)}{\partial t} \right)_{\text{coalescence}} = \frac{1}{2} \int_0^m K_W(m-m', m') W(m-m', t) W(m', t) dm' - \int_0^{\infty} K_W(m, m') W(m, t) W(m', t) dm'. \quad (3.3)$$

In eq. (3.3),  $K_W(m, m')$  is the coalescence coefficient for particles of sizes  $m$  and  $m'$ ; the first integral accounts for the rate of formation of drops of size  $m$  from smaller drops, and the second integral accounts for the rate at which drops of size  $m$  coalesce with other drops, and hence for their rate of loss.

### Coagulation

Coagulation is essentially a coalescence process of which the protagonists are the ice particles; accordingly,

$$\left(\frac{\partial H(m,t)}{\partial t}\right)_{\text{coagulation}} = \frac{1}{2} \int_0^m K_H(m-m',m')H(m-m',t)H(m',t)dm' - \int_0^\infty K_H(m,m')H(m,t)H(m',t)dm', \quad (3.4)$$

where  $K_H(m,m')$  is the coagulation coefficient for ice particles of sizes  $m$  and  $m'$ .

### Riming

The process of riming affects both the ice and the water distributions. The rate of change in the spectrum of ice particles is given by

$$\left(\frac{\partial H(m,t)}{\partial t}\right)_{\text{riming}} = \int_0^m K_R(m-m',m')H(m-m',t)W(m',t)dm' - \int_0^\infty K_R(m,m')H(m,t)W(m',t)dm' \quad (3.5)$$

where  $K_R(m,m')$  is the riming coefficient. The first integral on the right accounts for the rate of formation of ice particles of size  $m$  from collision of ice particles and water droplets of smaller sizes. The second term accounts for the rate of loss of ice particles of size  $m$  due to riming.

The rate of change in the spectrum of water drops produced

by the riming process is:

$$\left( \frac{\partial W(m,t)}{\partial t} \right)_{\text{riming}} = - \int_0^{\infty} K_R(m,m') W(m,t) H(m',t) dm' \quad (3.6)$$

### Accretion

The rate of growth of a spherical ice particle of mass  $m_h$  that is accreting matter from the vapor phase has been expressed by Byers (1965) as

$$\frac{dm_h}{dt} = \frac{4\pi r_h \left( \frac{p - p_h}{p_h} \right)}{\frac{L_s^2 M_w}{kRT^2} + \frac{RT}{DM_w p_h(T)}} = \frac{4\pi r_h \left( \frac{p - p_h}{p_h} \right)}{A + B} \quad (3.7)$$

where  $p$  is the ambient water vapor density,  $p_h$  is the vapor density above an ice particle,  $L_s$  is the latent heat of sublimation,  $k$  is the thermal conductivity of air,  $M_w$  is the molecular weight of water,  $D$  is the diffusivity of water vapor in air, and  $p_h(T)$  is the saturation vapor pressure around an ice particle at temperature  $T$ .

To separate the mass dependence from the temperature and time dependence, eq. (3.7) may be written as

$$\frac{dm_h}{dt} = G(T,t) \theta(m_h) \quad (3.8)$$

where

$$G(T, t) = \frac{4\pi(3/4 \rho_2)^{1/3}}{A + B} \left( \frac{p - p_h}{\rho_h} \right) \quad (3.9)$$

and

$$\theta(m_h) = m_h^{1/3}$$

The rate of change in the spectrum of the ice particles due to the accretion process can accordingly be written as

$$\left( \frac{\partial N(m, t)}{\partial t} \right)_{\text{accretion}} = - \frac{\partial (G(T, t) m^{1/3})}{\partial m} \quad (3.10)$$

### Evaporation

The evaporation rate from the surface of a water drop can similarly be expressed as

$$\frac{dm_w}{dt} = U(T, t) \theta(m_w) \quad (3.11)$$

where

$$U(T, t) = \frac{4\pi(3/4 \rho_2)^{1/3}}{\frac{L_v M_w}{kRT^2} + \frac{RT}{D M_w p_w(T)}} \left( \frac{p - p_w}{p_w} \right) \quad (3.12)$$

and  $\theta(m_w) = m_w^{1/3}$

Here,  $L_v$  is the latent heat of vaporization and  $p_w(T)$  is the vapor pressure around a water droplet at temperature  $T$ .

Evaporation affects the distribution of water drops in another way: As a water drop becomes smaller and smaller due to vaporization, it will ultimately shrink to a size  $m_1$ , at which we can no longer consider as part of the water drop population but rather as part of the vapor phase. The resulting change in the water drop population is:

$$-W(m, t) U(T, t) m^{1/3} \delta(m - m_1)$$

where  $\delta$  is the unit impulse function. In our numerical computations  $m_1$  was taken to be  $0.5\mu$ .

The total rate of change in the water drop distribution produced by evaporation is accordingly

$$\left( \frac{\partial W(m, t)}{\partial t} \right)_{\text{evaporation}} = \frac{\partial (U(T, t) m^{1/3})}{\partial m} - W(m, t) U(T, t) m^{1/3} \delta(m - m_1). \quad (3.13)$$

### Nucleation

Recent work (Weickmann et al. (1970), Berg et al. (1968)) shows that the conversion of water drops to ice by silver iodide occurs primarily via contact nucleation with contact occurring

via Brownian diffusion. The rate at which water drops of size  $m$  are converted to ice particles by this mechanism is

$$4\pi D_p r_w W(m, t) n_f$$

where  $D_p$  is the diffusivity of silver iodide aerosol and  $n_f$  is the number concentration of the silver iodide particles.

Since the ice particles are regarded as spherical, we can write

$$\left( \frac{\partial H(m, t)}{\partial t} \right)_{\text{nucleation}} = - \left( \frac{\partial W(m, t)}{\partial t} \right)_{\text{nucleation}} = Q n_f m^{1/3} W(m, t) \quad (3.14)$$

where  $Q = 4\pi D_p (3/4\pi \rho_i)^{1/3}$

The radii of aerosol particles used for seeding generally vary between  $0.01 \mu$  and  $0.1 \mu$ . We will accordingly consider the radius of the seed particles to be  $0.05 \mu$ . The number of aerosol particles that lead to formation of ice particles by contact nucleation is but a small fraction of the total number,  $n_f$ , of seed particles;  $n_f$  shall therefore be regarded as a constant (Slinn, 1971).

One can now assemble eqs. (3.1) and (3.2). We shall, however, spare the reader the sight of two very long and cumbersome expressions, and this accordingly brings to conclusion the formulation of the model.

### 3.3 CHOICE OF COLLECTION COEFFICIENTS

Apart from initial conditions, solution of eqs. (3.1) and (3.2) depends upon the nature of the collection coefficients  $K_W(m,m')$ ,  $K_H(m,m')$  and  $K_R(m,m')$ , and these are not easy to ascertain.

Most investigators have assumed the coalescence of water drops to occur solely as a result of gravitational effects (i.e., different fall velocities of drops of different sizes).  $K_W(m,m')$  has accordingly been formulated upon this mechanism. Saffman and Turner (1956), however, have shown that turbulent effects cannot be ignored in  $K_W(m,m')$  for most types of clouds, and  $K_W(m,m')$  based only on gravitational coalescence will result in fundamental errors.

While much effort has been devoted to the determination of  $K_W(m,m')$ , little has been done to elucidate the nature and magnitude of the coagulation coefficient,  $K_H(m,m')$ , and the riming coefficient,  $K_R(m,m')$ . Ryan, for example, ignored ice coagulation altogether, and took  $K_R(m,m')$  and  $K_W(m,m')$  to be identical; the latter assumption appears to be consistent with our view of the ice particle as spherical and of density of  $1 \text{ gm/cm}^3$ . On the other hand, we should note that Takeda (1968) has shown that there is a considerable difference between the growth rates of a plate-like crystal and a spherical ice particle

in a supercooled cloud.

Since adequate descriptions of  $K_W(m, m')$ ,  $K_H(m, m')$  and  $K_R(m, m')$  are not available, we have adopted expressions that are widely used in the analysis of particle growth in coalescing systems. We have used constant collection coefficients and collection coefficients which are proportional to the sum of the masses. Golovin (1963) has shown that the latter approximation is a reasonable choice for turbulent coalescence and electrostatic coalescence as well as for gravitational coalescence. Golovin's sum-of-the-masses coalescence coefficient is:

$$K_W(m, m') = \frac{b}{\rho_l} E(m + m') = b' E(m + m')$$

where  $E$  is the entrainment coefficient,  $\rho_l$  is the density of liquid water, and  $b \approx 6 \times 10^3 \text{ sec}^{-1}$  when the radii of the colliding droplets exceed  $25 \mu$ . When the colliding droplets have radii in the range of  $10 \mu$  to  $25 \mu$ ,  $b$  varies between  $1.2 \times 10^3 \text{ sec}^{-1}$  and  $6 \times 10^3 \text{ sec}^{-1}$ .

We expect the collection coefficients for coagulation and riming to differ from the collection coefficient for coalescence. Accordingly, we have defined  $E_R$  and  $E_H$  to be the entrainment coefficients for riming and coagulation, respectively. Following Golovin we have assumed the entrainment coefficient for coalescence to equal 1. For convenience, we have tabulated below all the

collection coefficients which find expression in this work.

---

<u>Collection coefficients</u>			
<u>Process</u>	<u>General expression</u>	<u>Constant coefficient</u>	<u>sum-of-the-masses coefficient</u>
Coalescence	$K_W(m, m')$	$K_W$	$b'(m+m')$
Coagulation	$K_H(m, m')$	$K_H$	$b'E_H(m+m')$
Riming	$K_R(m, m')$	$K_R$	$b'E_R(m+m')$

---

Table 3.1. Collection Coefficients

We shall presently proceed to cast eqs. (3.1) and (3.2) into dimensionless quantities, and form equations in the moments of the distributions. The moment equations will be solved and analyzed using constant collection coefficients. In a few specific cases, these solutions will be compared to the corresponding solutions for the more physically realistic sum-of-the-masses coefficients.

### 3.4 THE DIMENSIONLESS EQUATIONS

We introduce the following dimensionless variables:

$$\begin{aligned}
 y &= \frac{N_0}{M_0} m \\
 x &= \frac{N_0}{M_0} m' \\
 h(y, \tau) &= \frac{M_0}{N_0^2} H(m, t) \\
 w(y, \tau) &= \frac{M_0}{N_0^2} W(m, t) \\
 B(T, t) &= \frac{G(T, t)}{D\rho_0^{2/3}} \\
 A(T, t) &= -\frac{U(T, t)}{D\rho_0^{2/3}}
 \end{aligned} \tag{3.16}$$

where  $N_0$  and  $M_0$  are, respectively, the initial number concentration and mass density of the water drops, and  $\rho_0$  is the initial mass density of the water vapor. Corresponding to the two types of collection coefficients, we have two different expressions for the dimensionless time: For a constant collection coefficient,

$$\tau = K_R N_0 t \quad (3.17a)$$

and when sum-of-the-masses coefficients are used,

$$\tau = \frac{b' E_R t}{\rho_\lambda} \quad (3.17b)$$

Substituting the dimensionless variables into eqs. (3.1) and (3.2), we get for the ice balance

$$\begin{aligned} & \frac{\partial h(y, \tau)}{\partial \tau} + \alpha B(T, \tau) \frac{\partial y^{1/3} h(y, \tau)}{\partial y} \\ &= y^i \int_0^Y h(y-x, \tau) w(x, \tau) dx \\ &+ \frac{\alpha y^i}{2} \int_0^Y h(y-x, \tau) h(x, \tau) dx - \beta h(y, \tau) \int_0^\infty (y+x)^i h(x, \tau) dx \\ &- h(y, \tau) \int_0^\infty (y+x)^i w(x, \tau) dx \\ &+ \psi y^{1/3} w(y, \tau) \end{aligned} \quad (3.18)$$

and the dimensionless water balance is:

$$\begin{aligned}
& \frac{\partial w(y, \tau)}{\partial \tau} - \alpha A(T, \tau) \frac{\partial y^{1/3} w(y, \tau)}{\partial y} \\
&= \frac{\nu y^i}{2} \int_0^y w(y-x, \tau) w(x, \tau) dx = \int_0^\infty (y+x)^i w(y, \tau) h(x, \tau) dx \\
&- \nu w(y, \tau) \int_0^\infty (y+x)^i w(x, \tau) dx - \alpha A(T, \tau) y^{1/3} w(y, \tau) \delta(y-y_1) \\
&- \psi y^{1/3} w(y, \tau). \tag{3.19}
\end{aligned}$$

In eqs. (3.18) and (3.19)  $i = 0$  when constant collection coefficients are used, and  $i = 1$  when the coefficients are proportional to the sum of the masses. The dimensionless groups  $\alpha$ ,  $\psi$ ,  $\beta$  and  $\gamma$  are defined in Table 3.2 below.

Collection Coefficients	Dimensionless Groups			
	$\alpha$	$\psi$	$\beta$	$\gamma$
Constant	$D P_o^{2/3}$	$Q n_f M_o^{1/3}$	$K_H$	$K_W$
	$K_R N_o^{1/3} M_o^{2/3}$	$K_R N_o^{4/3}$	$K_R$	$K_R$
Sum-of-the-masses	$D P_o^{2/3} N_o^{2/3}$	$Q n_f$	$E_H$	$1$
	$b' E_R M_o^{5/3}$	$b' E_R M_o^{2/3} N_o^{1/3}$	$E_R$	$E_R$

Table 3.2. Dimensionless Groups

We note that  $\alpha_B(T, \tau)$  and  $\alpha_A(T, \tau)$  are roughly ratios of the rate of diffusion to the rate of riming, and  $\psi$  is a rough measure of the ratio of the rate of contact nucleation to the rate of riming.

### 3.5 THE MOMENT EQUATIONS

Eqs. (3.18) and (3.19) are too formidable to allow analytical solutions, and numerical solutions tend to be tedious and may be inexact (Long, 1971, and Drake, 1972). For the purpose at hand, however, it is not necessary to know how the distributions vary with time; it is sufficient that we follow the evolution in time of the moments of the distributions.

The  $n$ th moments of the two distributions are,

$$Y_n(\tau) = \int_0^{\infty} y^n h(y, \tau) dy \quad (3.20)$$

$$M_n(\tau) = \int_0^{\infty} y^n w(y, \tau) dy. \quad (3.21)$$

Multiplying eqs. (3.18) and (3.19) by  $y^n dy$  and integrating from 0 to  $\infty$ , we obtain the differential equations that govern the moments of the two distributions. For the ice particles,

$$\begin{aligned}
\frac{dY_n}{d\tau} &= n \alpha B(T, \tau) Y_{n-2/3} + \sum_{l=0}^{n+i} \binom{n+i}{l} Y_{n+i-l} \mu_l \\
&+ \frac{A}{2} \sum_{l=0}^{n+i} \binom{n+i}{l} Y_{n+i-l} Y_l - B \sum_{j=0}^i Y_{n+j} Y_{i-j} \\
&- \sum_{j=0}^i Y_{n+j} M_{i-j} + \psi \mu_{n+1/3}
\end{aligned} \tag{3.22}$$

and for the water drops

$$\begin{aligned}
\frac{d\mu_n}{d\tau} &= -n \alpha A(T, \tau) \mu_{n-2/3} + \frac{\gamma}{2} \sum_{l=0}^{n+i} \binom{n+i}{l} \mu_{n+i-l} \mu_l \\
&- \sum_{j=0}^i \mu_{n+j} Y_{i-j} - \nu \sum_{j=0}^i \mu_{n+j} M_{i-j} \\
&- \alpha w(y_1, \tau) A(T, \tau) y_1^{n-1/3} - \psi \mu_{n+1/3}.
\end{aligned} \tag{3.23}$$

Again,  $i=0$  for constant collection coefficients, and  $i=1$  when sum-of-the-masses coefficients are used.

Having assumed no inflow or outflow of mass, it follows that

$$\rho(\tau) = \rho_0 + [\mu_1(0) - \mu_1(\tau) - Y_1(\tau)]M_0. \quad (3.24)$$

We also note that expressions for  $A(T, \tau)$  and  $B(T, \tau)$  can be obtained in terms of the moments by using eq. (3.24) in conjunction with eqs. (3.5), (3.6) and (3.16).

Using eqs. (3.22) and (3.23), we list below the equations for the zeroth, first, and second moments of the solid and liquid distributions. For the ice:

$$\frac{\partial Y_0}{\partial \tau} = -\frac{\beta}{2} Y_0 Y_i + \psi M_{1/3}$$

$$\frac{\partial Y_1}{\partial \tau} = \alpha B(T, \tau) Y_{1/3} + \sum_{j=0}^i Y_j M_{i-j+1} + \psi M_{4/3} \quad (3.25)$$

$$\frac{\partial Y_2}{\partial \tau} = 2\alpha B(T, \tau) Y_{4/3} + Y_0 M_{i+2} + \sum_{j=1}^{i+1} (3+i-j) Y_j M_{i-j+2}$$

$$+ \beta(i+1) Y_1 Y_{i+1} + \psi M_{7/3}.$$

And for the water drops:

$$\frac{\partial M_0}{\partial \tau} = - \sum_{j=0}^i \gamma_j M_{i-j} - \sqrt{\frac{i+1}{2}} M_0 M_i - \alpha A(T, \tau) w(y_1, \tau) y_1^{1/3} - \psi M_{1/3}$$

$$\begin{aligned} \frac{\partial M_1}{\partial \tau} = & - \alpha A(T, \tau) M_{1/3} - \sum_{j=0}^i M_{j+1} \gamma_{i-j} - \alpha A(T, \tau) w(y_1, \tau) y_1^{4/3} \\ & - \psi M_{4/3} \end{aligned} \quad (3.26)$$

$$\begin{aligned} \frac{\partial M_2}{\partial \tau} = & -2 \alpha A(T, \tau) M_{4/3} + \sqrt{(i+1)} M_1 M_{i+1} \\ & - \sum_{j=0}^i M_{i+2-j} \gamma_{ij} - \alpha A(T, \tau) w(y_1, \tau) y_1^{7/3} - \psi M_{7/3}. \end{aligned}$$

Assuming that initially no ice particles are present, we have

$$\gamma_0(0) = \gamma_1(0) = \gamma_2(0) = 0$$

$$M_0(0) = M_1(0) = 1$$

and  $M_2(0)$  depends on the initial distribution.

Eqs. (3.25) and (3.26) are not self-contained. To solve these equations we need expressions for the fractional moments and  $w(y_1, \tau)$  which, of course, are themselves dependent upon the unknown distributions  $w(y, \tau)$  and  $h(y, \tau)$ . Hulburt and Katz (1964) suggested the use of orthogonal polynomials to approximate the distributions. This method, unfortunately, leads to difficulties because of improper expansions (Hulburt, Bayewitz and Shinnar (1975)). We have accordingly adopted non-orthogonal fitting functions which closely approximate the whole solution over the whole time. Fitting functions of this type have been used by Klepfer, Sonshine and Shinnar (1969). This method is applicable when the solution approaches a self-preserving distribution. The way these functions are chosen, and a procedure for checking their validity will be illustrated in a subsequent section.

We have examined two types of clouds, continental and maritime, and have found it necessary to select three different sets of distributions: When collection coefficients were regarded as constants, the functions chosen for  $w(y, \tau)$  and  $h(y, \tau)$  applied to both continental and maritime clouds, but when sum-of-the-masses coefficients were used, different distributions were adopted for the continental and the maritime clouds.

(i) Constant collection coefficients.

The distributions chosen are of the form,

$$w(y, \tau) = \frac{(\lambda_w y/a_w)^{\lambda_w} \mu_0 \exp(-\lambda_w y/a_w)}{y^{\Gamma}(\lambda_w)} \quad (3.27a)$$

$$h(y, \tau) = \frac{(\lambda_h y/a_h)^{\lambda_h} \gamma_0 \exp(-\lambda_h y/a_h)}{y^{\Gamma}(\lambda_h)} \quad (3.27b)$$

where

$$a_w = \mu_1/\mu_0 \quad ; \quad \lambda_w = \frac{a_w^2}{\mu_2/\mu_0 - a_w^2}$$

and

$$a_h = \gamma_1/\gamma_0 \quad ; \quad \lambda_h = \frac{a_h^2}{\gamma_2/\gamma_0 - a_h^2}$$

These distributions satisfy eqs. (3.20) and (3.21) for  $n = 0, 1, 2$ . It is interesting to note that eq. (3.27a) is the solution obtained by Scott (1968) for a process of pure coalescence,  $\partial W/\partial t = (\partial W/\partial t)$  coalescence, with  $K_w = \text{constant}$  and  $w(y, 0) = e^{-y}$ .

Using the distributions of eq. (3.27), we obtain expressions for the fractional moments:

$$\mu = \int_{\frac{n}{3}}^{\infty} y^{n/3} w(y) dy = \frac{\mu_0 \Gamma(\lambda_w + \frac{n}{3})}{(\lambda_w/a_w)^{n/3} \Gamma(\lambda_w)} \quad (3.28a)$$

$$\gamma = \int_{\frac{n}{3}}^{\infty} y^{n/3} h(y) dy = \frac{\lambda_0 \Gamma(\lambda_h + \frac{n}{3})}{(\lambda_h/a_h)^{n/3} \Gamma(\lambda_h)} \quad (3.28b)$$

(ii) Sum-of-the-masses collection coefficients; Maritime clouds.

Maritime and continental clouds differ essentially in that the former contains initially larger droplets. The average droplet size initially in a maritime cloud is typically  $20 \mu$ ; the corresponding value for the continental cloud is only  $9 \mu$ . Accordingly, diffusional growth is relatively unimportant in the evolution of a seeded maritime cloud. When sum-of-the-masses coefficients are used and the extent of growth of diffusional processes is small, Golovin (1965) has recommended use of distributions of the form,

$$h(y, \tau) = \frac{\gamma_0 e^{-\eta_h y}}{\eta_h - \sqrt{\eta_h^2 - \epsilon_h^2}} \frac{I_1(\epsilon_h y) e^{-\eta_h y}}{y} \quad (3.29a)$$

and

$$w(y, \tau) = \frac{\mu_0 \epsilon_w}{\eta_w \sqrt{\eta_w^2 - \epsilon_w^2}} \frac{I_1(\epsilon_w y) e^{-\eta_w y}}{y} \quad (3.29b)$$

where  $I_1$  is the modified Bessel function of the first kind,

$$\epsilon_h = \sqrt{\frac{\gamma_2 \gamma_0^3}{\gamma_1^4} \left( \frac{\gamma_2 \gamma_0}{\gamma_1^2} - 2 \right)}$$

$$\eta_h = \frac{\gamma_2 \gamma_0^2}{\gamma_1^3} - \frac{\gamma_0}{\gamma_1}$$

and  $\epsilon_w$  and  $\eta_w$  are similarly defined.

The fractional moments follow,

$$\begin{aligned}
 Y_{\frac{n}{3}} &= \int_0^{\infty} y^{\frac{n}{3}} h(y, \tau) dy \\
 &= \frac{\Gamma(1+\frac{n}{3}) V_0 \varepsilon_h^2}{2 \left( \eta_h - \sqrt{\varepsilon_h^2 - \eta_h^2} \right) \eta_h^{1+\frac{n}{3}}} F\left(1+\frac{n}{3}, \frac{n+3}{6}; 2; \frac{\varepsilon_h^2}{\eta_h^2}\right) \quad (3.30a)
 \end{aligned}$$

and

$$\begin{aligned}
 \mu_{\frac{n}{3}} &= \frac{\Gamma(1+\frac{n}{3}) \mu_0 \varepsilon_w^2}{2 \left( \eta_w - \sqrt{\varepsilon_w^2 - \eta_w^2} \right) \eta_w^{1+\frac{n}{3}}} F\left(1+\frac{n}{3}, \frac{n+3}{6}; 2; \frac{\varepsilon_w^2}{\eta_w^2}\right) \quad (3.30b)
 \end{aligned}$$

where  $F(a, b; c; z)$  is the hypergeometric function.

(iii) Sum-of-the-masses collection coefficients; continental clouds.

Collection and diffusional processes may be equally important in the evolution of continental clouds. Accretion produces a narrowing of the distribution of ice particles, while growth by coagulation causes the distribution to spread. Evaporation and growth by coalescence both widen the distribution of water drops. Since the

ice and water distributions are affected in different ways by the microphysical processes, and the relative importance of the processes change as particle growth proceeds, we have chosen different density functions to describe the distributions:

$$w(y, \tau) = \left(1 - \frac{0.5 \gamma_1}{\gamma_1 + \mu_1}\right) \frac{\mu_0}{\eta_w \sqrt{\eta_w^2 - \epsilon_w^2}} \frac{\epsilon_w}{y} I_1(\epsilon_w y) e^{-\eta_w y} +$$

$$\left(\frac{0.5 \gamma_1}{\gamma_1 + \mu_1}\right) \left(\frac{\lambda_w y}{a_w}\right)^{\lambda_w} \frac{\mu_0 \exp(-\lambda_w y/a_w)}{y \Gamma(\lambda_w)} : \mu_0 > 0.4 \quad (3.31a)$$

$$w(y, \tau) = (1 - \epsilon) \frac{\mu_0 \epsilon_w}{\eta_w \sqrt{\eta_w^2 - \epsilon_w^2}} \frac{I_1(\epsilon_w y) e^{-\eta_w y}}{y}$$

$$+ \epsilon \left(\frac{\lambda_w y}{a_w}\right)^{\lambda_w} \frac{\mu_0 \exp(-\lambda_w y/a_w)}{y \Gamma(\lambda_w)} : \mu_0 < 0.4 \quad (3.31b)$$

$$h(y, \tau) = \left(\frac{\lambda_h y}{a_h}\right)^{\lambda_h} \frac{\gamma_0 \exp(-\lambda_h y/a_h)}{y \Gamma(\lambda_h)} : \quad (3.31c)$$

where

$$\xi = \frac{0.5 \gamma_1 \Big|_{\mu_0 = 0.4}}{\gamma_1 \Big|_{\mu_0 = 0.4} + \mu_1 \Big|_{\mu_0 = 0.4}}$$

With the assumed density functions and the fractional moments thereof, eqs. (3.25) and (3.26) are now in closed form and may be solved for the zeroth, first, and second moments of the distributions. The validity of the assumed density functions, and hence the validity of the solutions to eqs. (3.25) and (3.26) may be checked by computing from eqs. (3.27), (3.29) and (3.31) the third, fourth, and if necessary higher moments of  $w(y, \tau)$  and  $h(y, \tau)$ , and comparing them to the corresponding values obtained from eqs. (3.22) and (3.23).

Following this procedure, we have used Hamming's modified predictor-corrector method to obtain numerical solutions of first order differential equations. Agreements within 5% for the third moments and within 15% for the fourth moments were obtained for the (1) ice distribution using constant collection coefficients, (2) ice distribution in maritime clouds using sum-of-the-masses coefficients, and (3) water distribution in continental clouds using sum-of-the-masses coefficients.

Differences in the third and fourth moments of the remaining distributions (water with constant coefficients; water with sum-of-the-masses coefficients in a maritime cloud; and ice with sum-of-the-masses coefficients in a continental cloud) increased slowly with the level of glaciation of the cloud. But even at 90% glaciation, the third moments differed by less than 30%. We do not think that the differences in the higher moments of the water distributions at 90% glaciation, when the water phase is practically depleted, have any real significance insofar as the accuracy of our results is concerned. As for the difference in the third and fourth moments of the ice distribution in a continental cloud, we note that in eq. (3.26), from which our solutions arise, the highest moment of the ice distribution is  $7/3$  and on that account we regard the accuracy of the solutions as only slightly affected.

### 3.6 SOLUTIONS - CONSTANT COLLECTION COEFFICIENTS

In our solutions,  $M_0$  was taken to be  $1 \text{ gm/cm}^3$  which is a typical value for both continental and maritime clouds. The second moment of the water distribution at time zero was assumed 2.45, and the seeding temperature and pressure were chosen, respectively, at  $-15^\circ\text{C}$  and 600 mm of Hg.

As noted in the introduction, we are primarily interested in following the evolution of large particles, ice and water, and accordingly the fraction of "available mass" present in particles of radii exceeding  $100\mu$ ,  $F(100\mu, \tau)$ , was computed as a function of time.  $F(100\mu, \tau)$  can be obtained from the ice and water distributions by

$$F(100\mu, \tau) = \frac{M_0 - \left( \frac{\int \bar{y}_w(y, \tau) dy}{146.7} + \frac{\int \bar{y}_h(y, \tau) dy}{146.7} \right)}{M_0 + \rho_w - \rho_i} \quad (3.32)$$

The "available mass" is defined here as the cloud's condensed mass at ice saturation,  $M_0 + \rho_w - \rho_H$ , and 146.7 is the dimensionless mass of a spherical particle 100 in radius and of density of  $1 \text{ gm/cm}^3$ .

In Fig. 3.1,  $F(100\mu, \tau)$  has been plotted as a function of the dimensionless time,  $\tau$ , for various values of  $\psi$ . Using curves of this kind, the dimensionless time,  $\tau_{0.6}$ ,

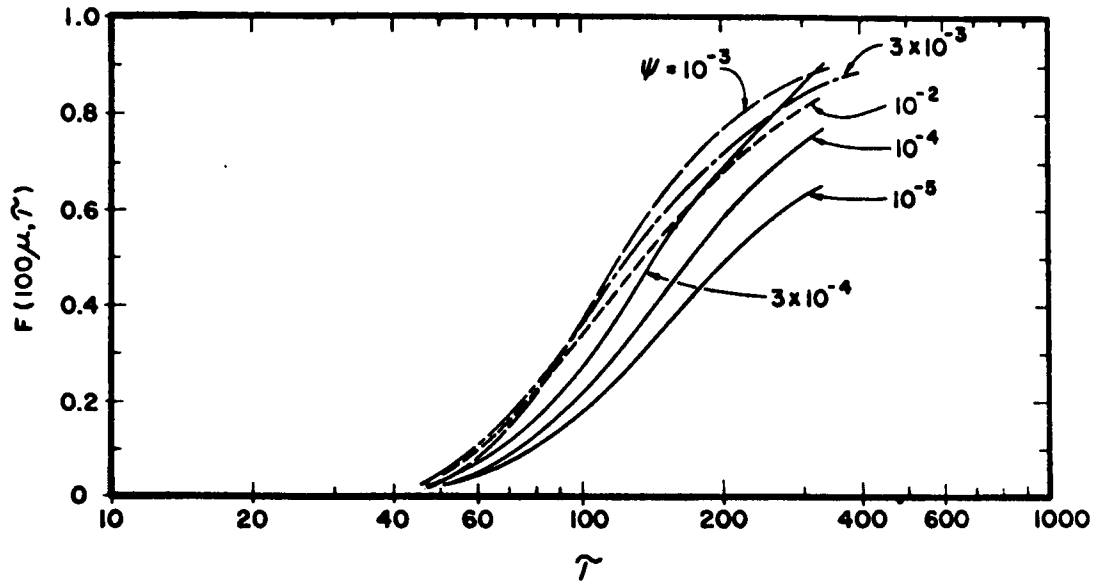


Fig. 3.1  $F(100\mu, \tau)$  vs. dimensionless time,  $\tau$ , for different values of  $\psi$ . Constant collection coefficients are in use, and  $\alpha B(T, 0) = 0.2$ ,  $A(T, 0) = 0$ ,  $\beta = 1.0$  and  $\nu = 1.0$ .

at which  $F(100\mu, \tau)$  reaches 0.6 is plotted against  $\psi$  for various values of  $\alpha_B(T, 0)$  in Fig. 3.2. The effects of

$\alpha_B(T, 0)$  and the seeding concentration,  $n_f$ , on the evolution of the cloud can perhaps be better understood from Fig. 3.3 where against  $n_f$  we have plotted the real time,  $t_{0.6}$ , it takes  $F(100\mu, \tau)$  to reach 0.6.

We note that the dependence of particle growth on the seeding concentration increases as  $\alpha_B(T, 0)$ , or the relative importance of diffusional growth, increases. This dependence is the result of the different amounts of mass that are available for diffusional growth at different seeding concentrations. While nearly  $(M_0 + \rho_w - \rho_H)$  gm/cm<sup>3</sup> may be transferred by diffusion when  $\alpha_B(T, 0)$  is large and the optimum seeding concentration is used, only  $\rho_w - \rho_H$  gm/cm<sup>3</sup> can be transferred when overseeding occurs and there is instant glaciation, and no mass can be transferred by diffusion when no seeding occurs.

We also note from Fig. 3.3 that the ratio of the optimum seeding concentration to the initial droplet concentration decreases from 10 to 0.3 as  $\alpha_B(T, 0)$  increases from 0.2 to 20.

The effect of seeding on the evolution of the cloud can be gauged by the ratio of the time at which  $F(100\mu, \tau)$

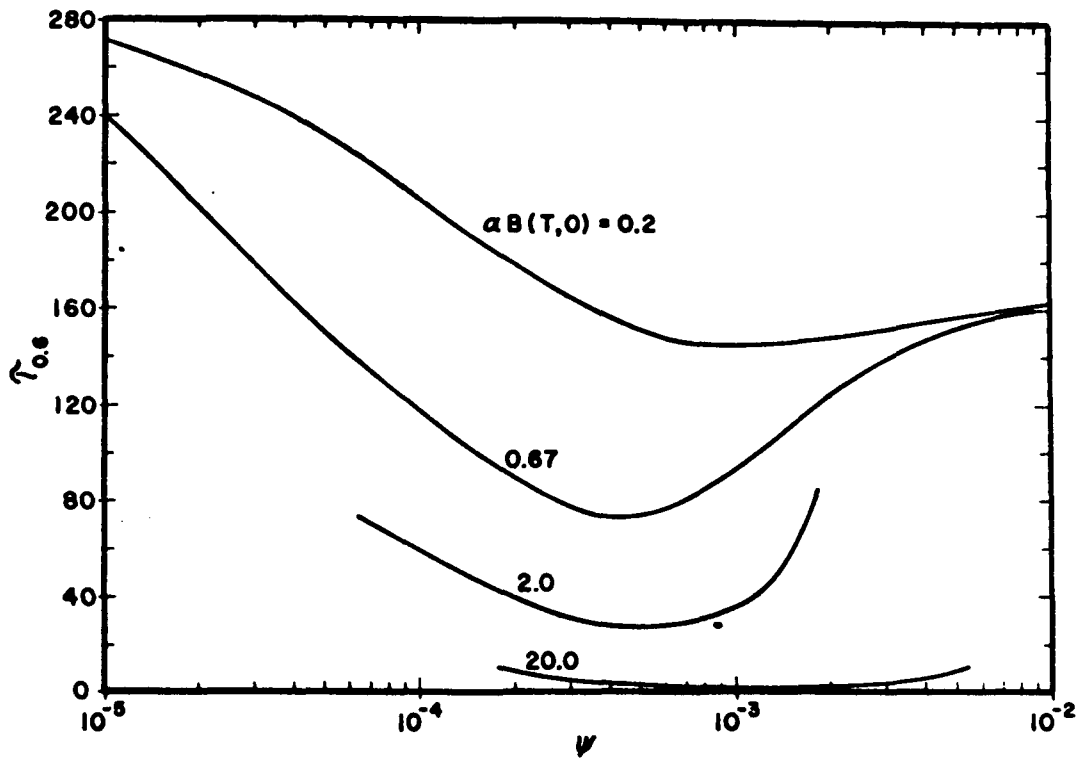


FIG. 3.2. Dimensionless time for  $F(100\mu, \tilde{\tau})$  to reach 0.6 as a function of  $\psi$ . Constant collection coefficients are in use, and  $\beta = 1$ ,  $\nu = 1$ ,  $A(T,0) = 0$ .

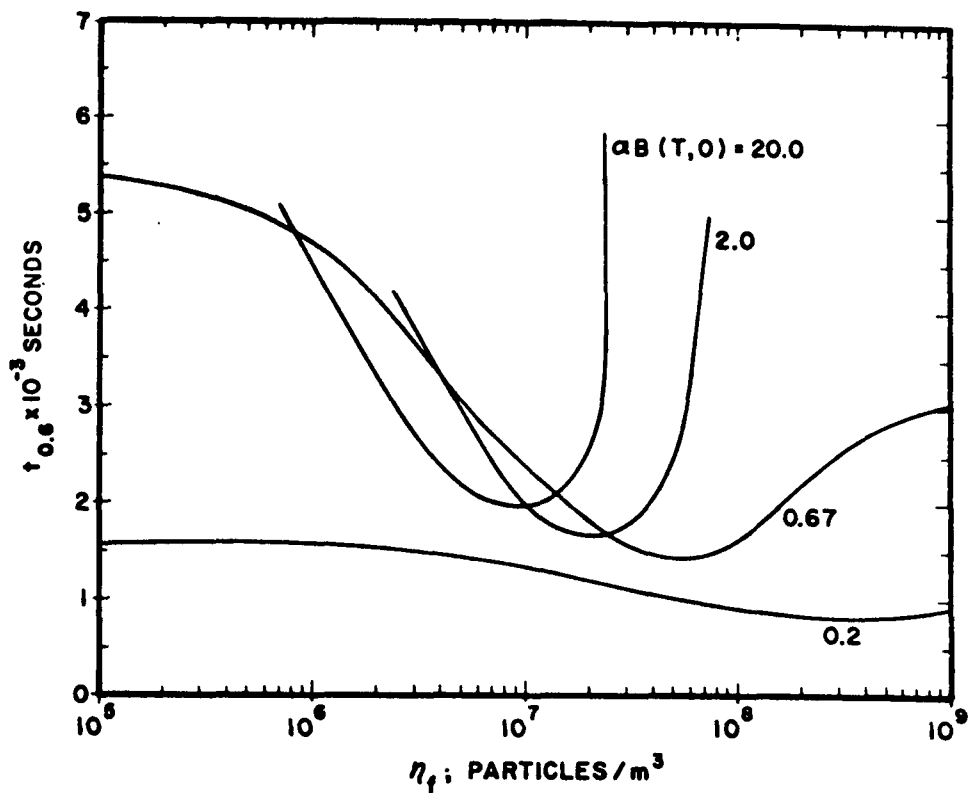


Fig. 3.3. The time,  $t_{0.6}$ , for  $F(100\mu, \gamma)$  to reach 0.6 as a function of the seeding concentration. Constant collection coefficients are in use, and  $\beta = 1$ ,  $\nu = 1$ ,  $A(T,0) = 0$ .

reaches 0.6 without seeding to the corresponding time when the optimum seeding concentration is used. We call this ratio the "seeding efficiency". Fig. 3.4 shows the variation of the seeding efficiency with  $\alpha_B(T,0)$ . Variations in  $\alpha_B(T,0)$  are largely the result of differences in the possible values which the constant riming coefficient may assume. Using the data of Danielsen, Bleck, and Morris (1972) for gravitational coalescence and assuming the riming and the coalescence coefficients to be equal, we find that the riming coefficient for a particle of 60  $\mu$ m and a particle of 15  $\mu$ m will make  $\alpha_B(T,0) = 0.2$  at  $-15^\circ\text{C}$  while the riming coefficient for a 30  $\mu$ m and an 8  $\mu$ m particle will make  $\alpha_B(T,0) = 20$  at  $-15^\circ\text{C}$ .

Seeding temperature also has an effect on  $\alpha_B(T,0)$ . At  $-15^\circ\text{C}$   $\alpha_B(T,0)$  is 25% greater than at  $-5^\circ\text{C}$  and growth at the lower temperature is thereof greater. The difference in the seeding efficiencies between maritime and continental clouds can be observed from Fig. 3.4 since  $\alpha_B(T,0)$  is generally about five times greater for continental clouds.

As mentioned previously, very little experimental data has been acquired for  $K_H(m,m')$  and  $K_R(m,m')$ . Hosler and Hallgren (1960) experimentally observed the coagula-

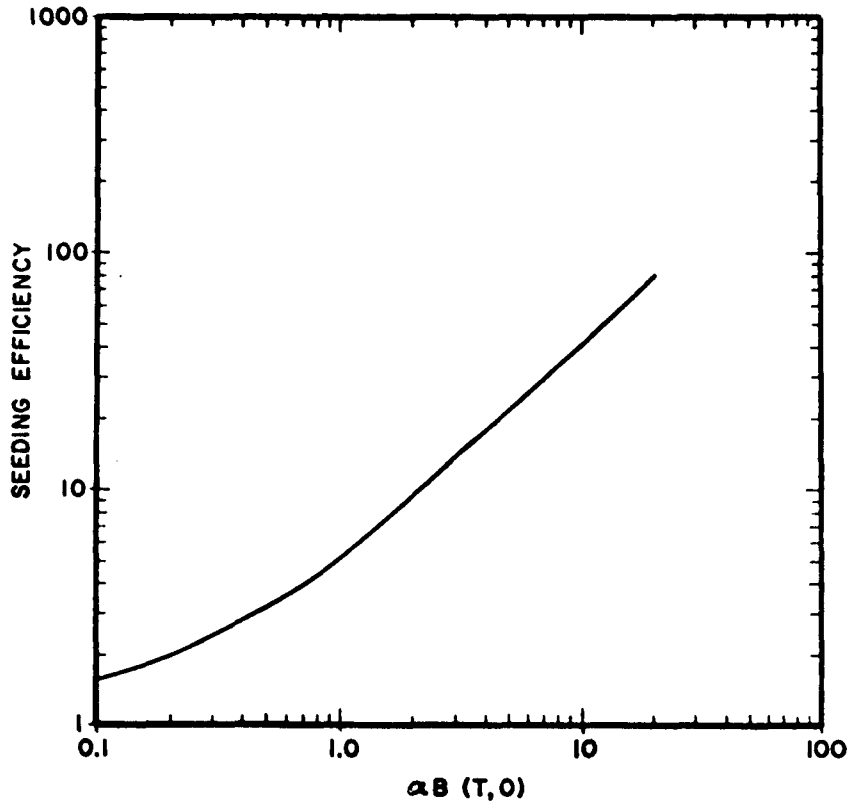


Fig. 3.4. Seeding efficiency vs.  $\alpha_B(T,0)$ . Constant collection coefficients are in use and  $\beta = 1$ ,  $\nu = 1$ ,  $A(T,0) = 0$ .

tion and growth of single ice particles of diameters of  $127\mu$  and  $360\mu$  that were introduced into clouds comprising ice particles of sizes in the range of  $7\mu$  to  $18\mu$ . The values which they found for  $K_H(m, m')$  were considerably less than corresponding values of  $K_W(m, m')$ . Since most investigators assume  $K_R(m, m')$  to be the same as  $K_W(m, m')$  we examined our equations when  $\beta$  assumes the value of 0.25, 0.5 and 10 and  $\nu$  equals to 0.5, 1.0, and 2.0. Fig.3.5 illustrates the results of overseeding for low values of  $\beta$  and Fig.3.6 shows the effect of  $\nu$  on particle growth at low seeding concentrations. It is interesting to note that the seeding efficiency is independent of  $\beta$ .

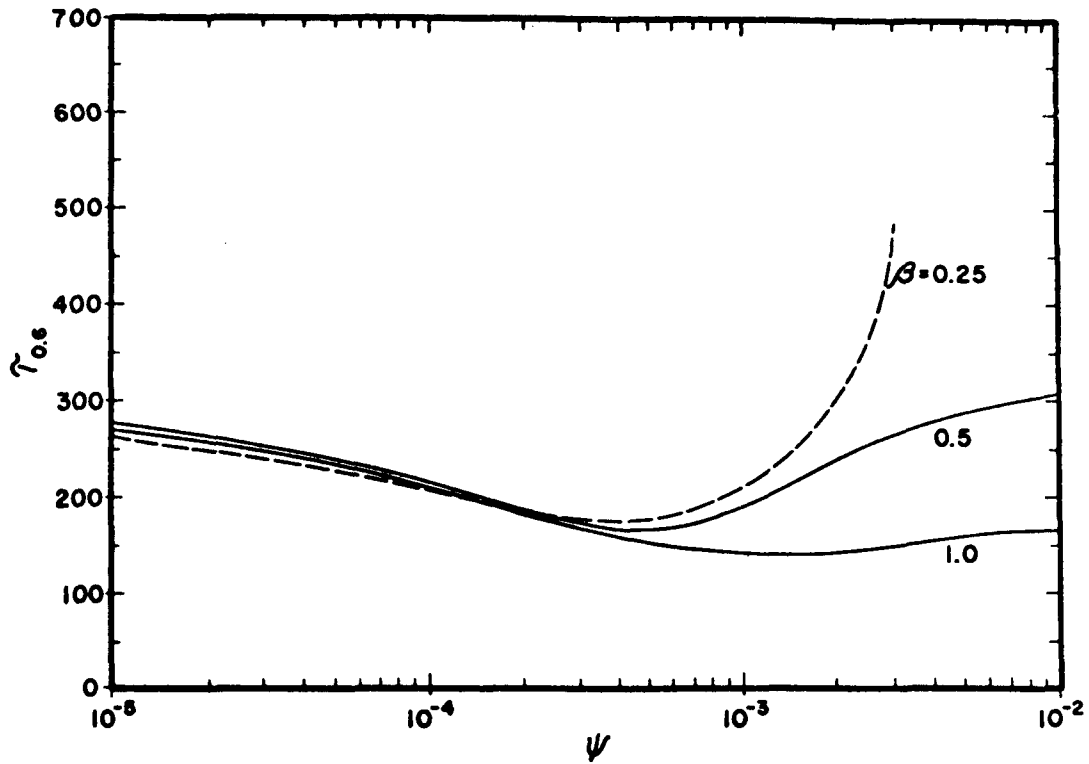


Fig. 3.5. Dimensionless time,  $\tau_{0.6}$ , for  $F(100\mu, \tau)$  to reach 0.6 as function of  $\psi$  for three values of  $\beta^3$ . Constant collection coefficients are in use, and  $\alpha_B(T, 0) = 0.2$ ,  $\nu = 1$ ,  $A(T, 0) = 0$ .

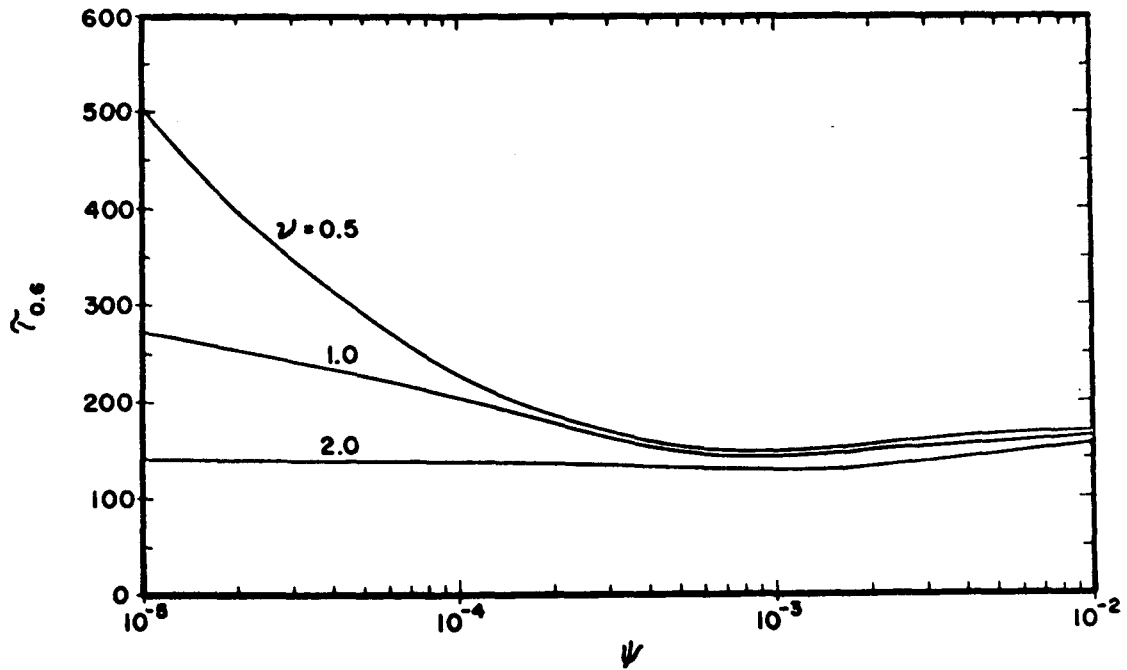


Fig. 3.6. Dimensionless time,  $\tau_{0.6}$ , for  $F(100\mu, \gamma)$  to reach 0.6 as a function of  $\psi$  for three values of  $\nu$ . Constant collection coefficients are in use, and  $\alpha B(T, 0) = 0.2$ ,  $A(T, 0) = 0$ ,  $\beta = 1$ .

### 3.7 SOLUTIONS - SUM-OF-THE-MASES COEFFICIENTS

We turn now to a description of the evolution of a seeded cloud using collection coefficients proportional to the sum of the masses of the interacting particles. Table 3.4 lists the initial distributions and moments for two continental clouds and for one maritime cloud. Note that the mass of an average droplet in a maritime cloud is an order of magnitude greater than the mass of an average droplet in a continental cloud. This difference is typical.

---

	$N_0$ $\text{cm}^{-3}$	$M_0$ $\text{gm}/\text{m}^3$	$m^2 W(m,t)$ $\frac{\text{gm}^2}{\text{m}^3}$	$w(y,0)$
continental cloud I	422	1.3	$8.85 \times 10^{-7}$	$\frac{3.17}{y} I_1(0.7y)e^{-1.22y}$
continental cloud II	422	1.3	$1.77 \times 10^{-6}$	$\frac{1.35}{y} I_1(3.29y)e^{-3.44y}$
maritime cloud	35	1.0	$1.93 \times 10^{-7}$	$\frac{1.19}{y} I_1(5.67y)e^{-5.75y}$

---

Table 3.4 Initial moments and distributions

Figure 3.7 shows the effect of seeding concentration on par-

ticle growth for continental cloud I for two values of  $q_B(T,0)$ , 40 and 20, corresponding to values of  $b'$  of  $3 \times 10^{-3}$  and  $6 \times 10^{-3} \text{ m}^3 \text{ gm}^{-1} \text{ sec}^{-1}$ , respectively. Once again we note that an increase in the collection rate - which amounts to a decrease in  $q_B(T,0)$  - shifts the optimum seeding concentration to a higher values and reduces the seeding efficiency. When  $q_B(T,0)$  is 40 the seeding efficiency is about 2, and seeding accordingly can promote the formation of rain. It is interesting to note that the ratio of the optimum seeding concentration to the initial droplet concentration lies between 0.8 and 5. For constant collection coefficients, this ratio is in the range of 0.3 to 10.

In Fig. 3.8 we have compared the evolution of the maritime cloud and continental cloud I. We note that seeding has a considerably larger effect on particle growth in the continental cloud, and that no optimum seeding concentration exists for the maritime cloud. Seeding in the maritime cloud only adds condensed mass to the particles as a result of the lower vapor density at ice saturation.

The extent to which particle growth is dependent upon the initial distribution was examined by using

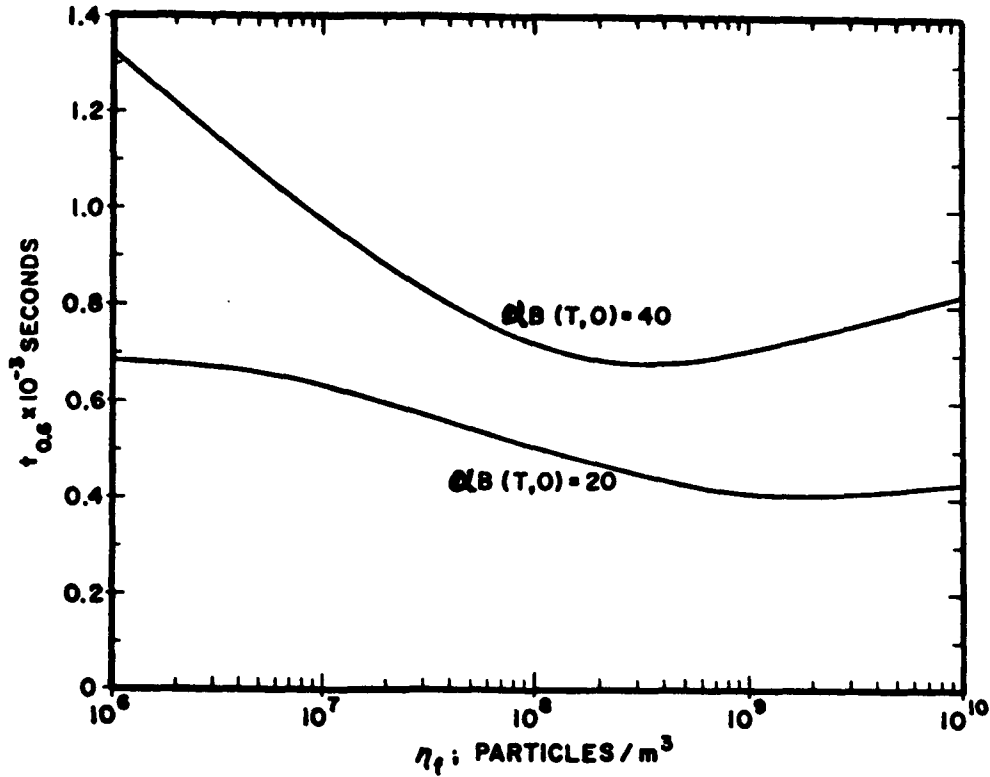


FIG. 3.7. The time,  $t_{0.6}$ , for  $F(100\mu, \tau)$  to reach 0.6 as a function of the seeding level. Sum-of-the-masses coefficients are in use and  $N_0 = 4.22 \times 10^8 \text{ m}^{-3}$ ,  $E_H = E_R = 1$ ,  $A(T,0) = 0$ . As  $n_f \rightarrow \infty$ ,  $t_{0.6}$  approaches 950 sec for  $\alpha B(T,0) = 40$ , and 490 sec for  $\alpha B(T,0) = 20$ .

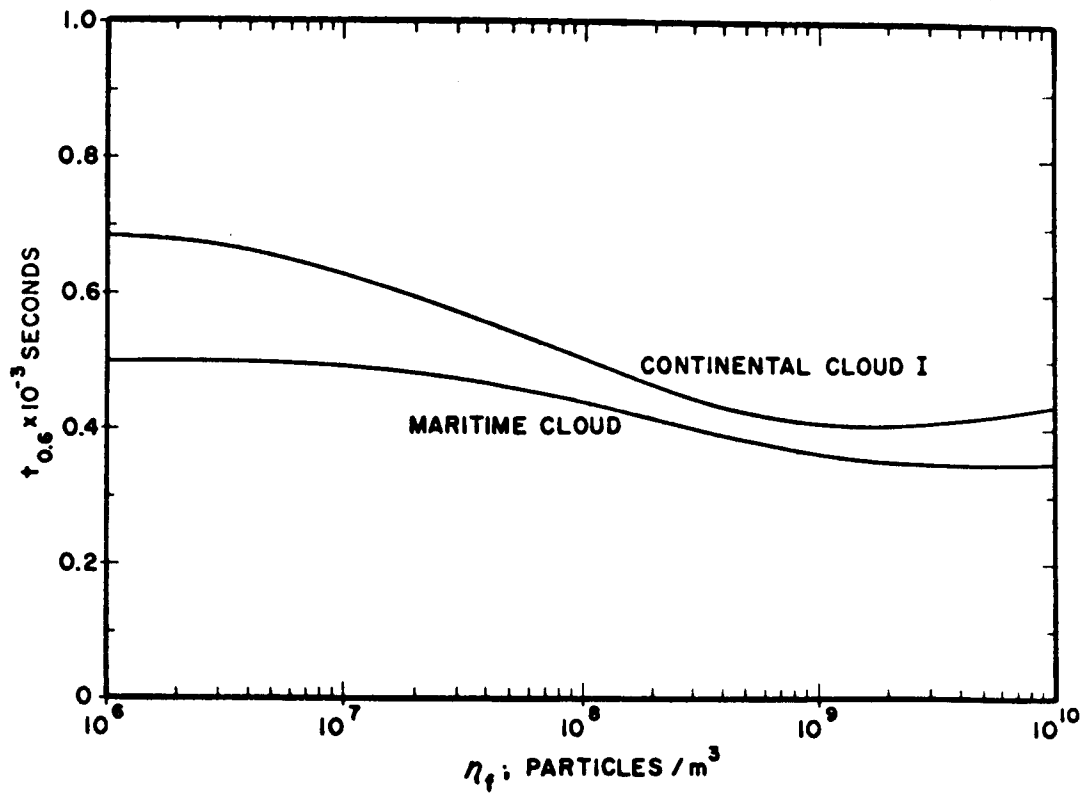


FIG. 3.8 The time,  $t_{0.6}$ , for  $F(100\mu, \tau)$  to reach 0,6 as a function of the seeding level for the maritime cloud and for continental cloud I. Sum-of-the-masses coefficients are in use and  $\alpha B(T,0) = 5.5$  for the maritime cloud,  $\alpha B(T,0) = 20$  for continental cloud I,  $E_H = E_R = 1$ ,  $A(T,0) = 0$ .

different values for the second moments at time zero. Using sum-of-the-masses collection coefficients we compared particle growth in continental clouds I and II whose second moments are initially 2.45 and 4.9, respectively. Fig. 3.9 shows that particle growth is slightly greater for the cloud with the wider initial distribution. The differences are more pronounced at low and very high levels of seeding where the relative importance of vapor accretion is small. The trends at low values of  $\psi$  are in qualitative agreements with Twomey's (1966) results for droplet growth in a warm cloud.

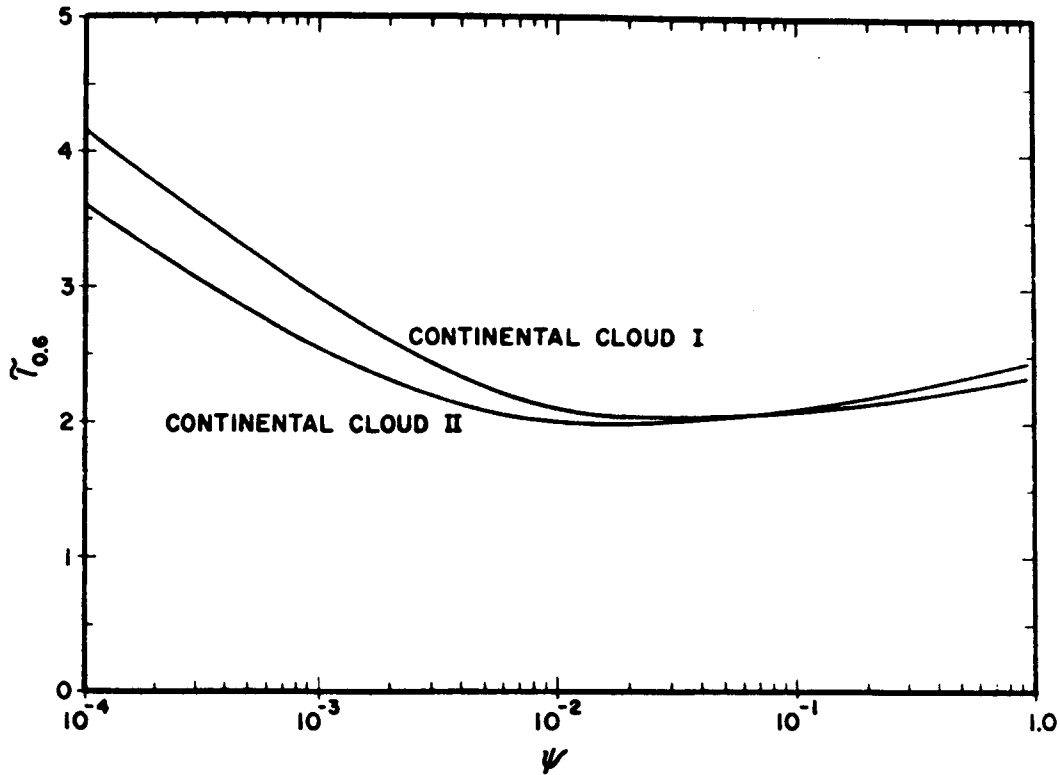


Fig. 3.9. Dimensionless time,  $\tau_{0.6}$ , for  $F(100\mu, \hat{\tau})$  to reach 0.6 as a function of  $\psi$  for continental clouds I and II. Sum-of-the-masses coefficients are in use and  $\alpha B(T,0) = 40$ ,  $E_H = E_R = 1$ ,  $A(T,0) = 0$ . As  $\psi \rightarrow \infty$ ,  $\tau_{0.6}$  approaches 3.0 and 2.75 for clouds I and II, respectively.

### 3.8 THE EFFECTS OF TEMPERATURE CHANGES DURING GLACIATION

So far we have considered clouds to be isothermal. Temperatures in a supercooled cloud, however, will in fact vary as a result of phase changes. The cloud temperature may be expressed as:

$$T(\tau) = T(0) + \frac{L_f}{C_p \rho_a} (M_0 (1 - u_1) + \rho(0) - \rho(\tau)) - \frac{L_v}{C_p \rho_a} (\rho(\tau) - \rho(0)); \quad \rho(\tau) < \rho(0) \quad (3.33a)$$

$$T(\tau) = T(0) + \frac{L_f M_0}{C_p \rho_a} (1 - u_1) + \frac{L_s}{C_p \rho_a} (\rho(0) - \rho(\tau)) ; \quad \rho(\tau) < \rho(0) \quad (3.33b)$$

In eqs. (3.33),  $L_f$  is the heat of fusion,  $L_v$  is the heat of vaporization,  $L_s$  is the heat of sublimation,  $C_p$  is the specific heat of the cloud, and  $\rho_a$  is the overall density of the cloud.

To get some feeling on the error incurred when isothermicity is assumed, we have computed particle growth in continental cloud I when the temperature is allowed to vary in accordance with eqs. (3.33) and compared the results to those obtained earlier for isothermal conditions. The comparison is shown in Fig. 3.10, and we note that sum-of-

the-masses coefficients have been used. We find that the error is practically nil for small values of  $\psi$ , and increases as  $\psi$  increases. Figs. 3.11 and 3.12 explain this trend. Fig. 3.11 shows that heating results in a slight increase in the density of the vapor in the cloud,  $\rho$ . This density increase corresponds to a decrease in the condensed mass available for growth by collection and accordingly the overall particle growth is retarded. Fig. 3.12 shows that the extent of glaciation increases with  $\psi$ . Since the amount of heat released during fusion is directly related to the per cent glaciation, the assumption of isothermicity incurs an error that increases with the extent of glaciation and with  $\psi$ .

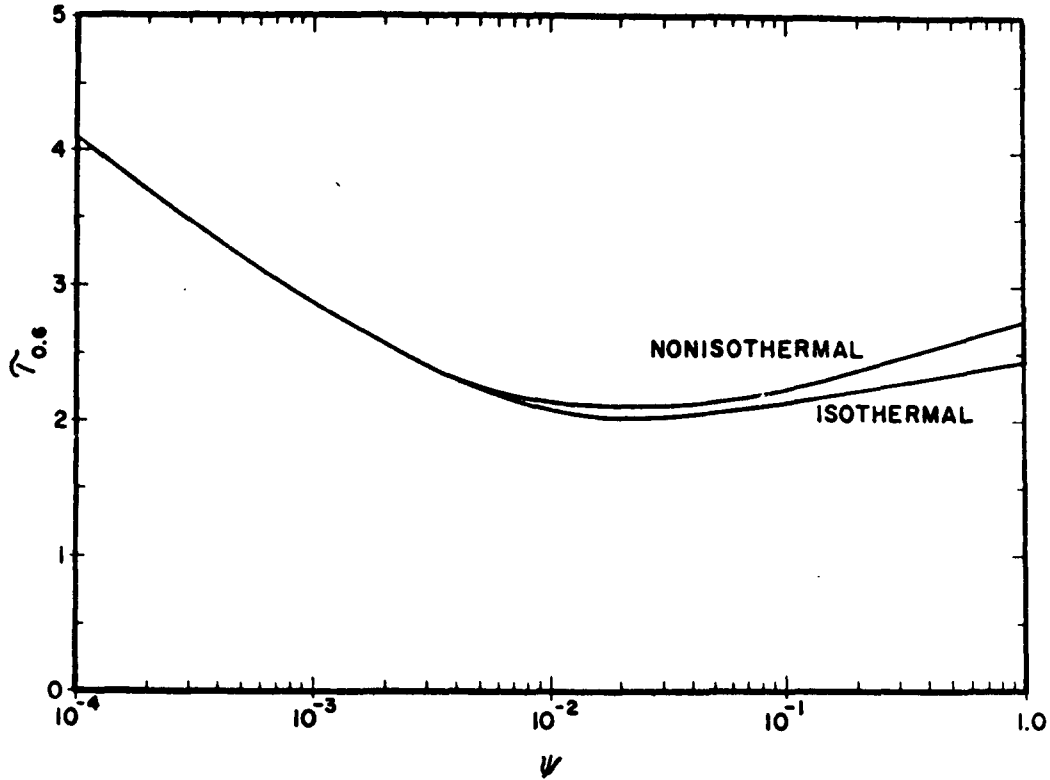


FIG. 3.10. Dimensionless time,  $\tau_{0.6}$ , for  $F(100\mu, \tau)$  to reach 0.6 as a function of  $\psi$  for continental cloud I under isothermal and nonisothermal conditions. Sum-of-the-masses coefficients are in use and  $\alpha B(T, 0) = 20$ ,  $A(T, 0) = 0$ ,  $E_H = E_R = 1$ . As  $\psi \rightarrow \infty$ ,  $\tau_{0.6}$  tends to 3.0 and 3.15 for the isothermal and nonisothermal clouds, respectively.

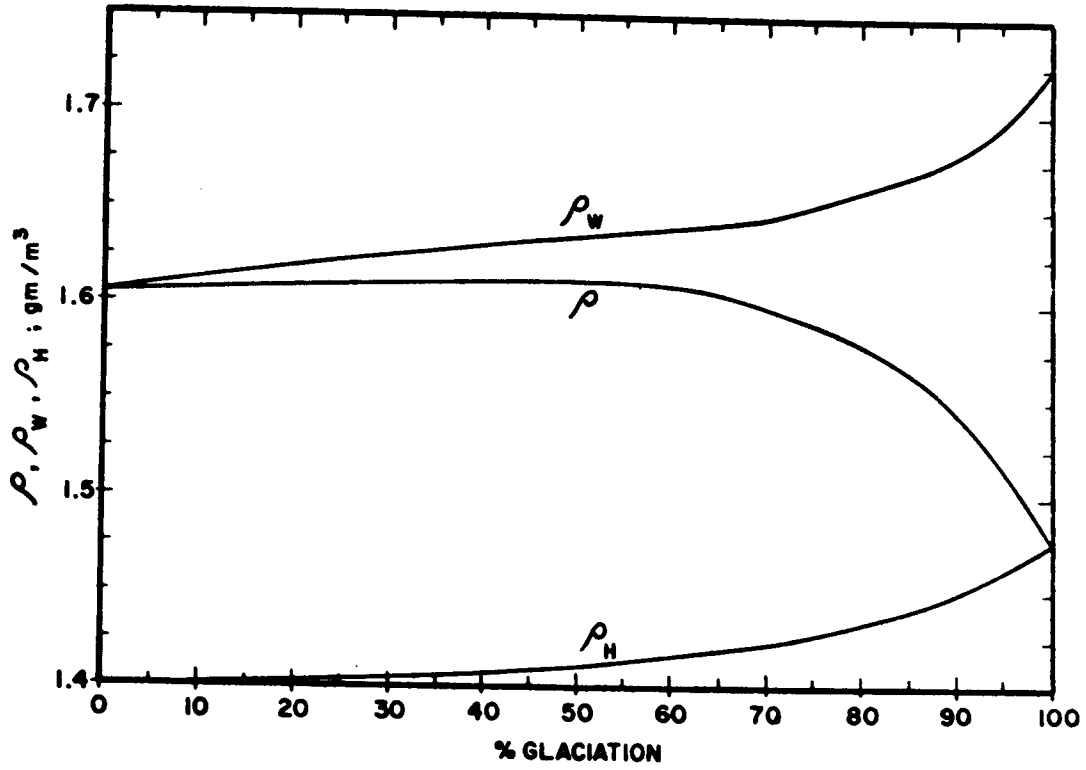


FIG. 3.11.  $\rho$ ,  $\rho_w$  and  $\rho_H$  vs. % glaciation for the nonisothermal cloud of Fig. 3.10.

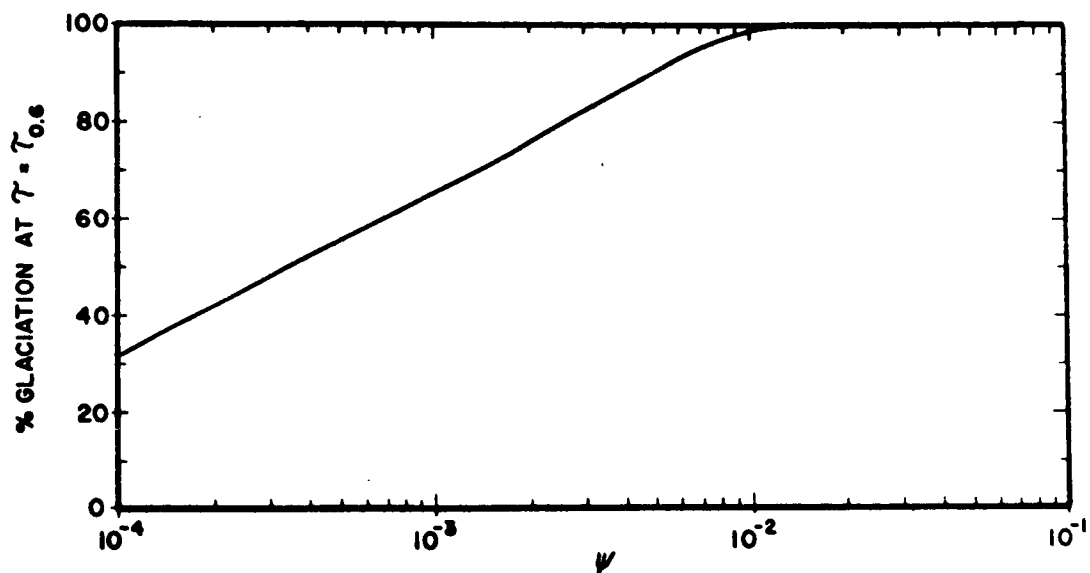


Fig. 3.12. Per cent glaciation at  $\tau = \tau_{0.6}$  as a function of  $\psi$  for the nonisothermal cloud of Fig. 3.10.

### 3.9 CONCLUSIONS

The evolution of seeded supercooled stationary clouds was simulated by a model which incorporates six microphysical processes affecting the distributions of ice particles and water drops. The model comprises material balances on the ice and water in the cloud, and is of the form of integro-differential equations in the water and ice distributions. These equations were solved for the first three moments of the distributions by using constant collection coefficients as well as coefficients proportional to the sum of the masses of the interacting particles. Nonisothermal effects were also examined.

Our objective was to gain understanding of the manner in which particle growth in the seeded cloud is affected by various parameters. We determined the following:

- (1) Seeding may significantly promote the overall growth of particles in a supercooled continental cloud. Seeding has only a small effect on overall particle growth in a supercooled maritime cloud.
- (2) The optimum seeding concentration is of the same order as the initial concentration of water drops. The optimum seeding concentration is

lower for clouds having a smaller average droplet mass initially.

- (3) The seeding efficiency stands in inverse proportions to the average droplet mass initially.
- (4) The degree of spread of the initial drop distribution has only a small effect on particle growth in the seeded cloud.
- (5) Neglecting dynamic effects, heat released during glaciation does not change appreciably the course of particle growth in the seeded cloud.
- (6) Qualitative results obtained using constant collection coefficients are very similar to results obtained using the more physically realistic sum-of-the-masses coefficient.

APPENDIX ASolution of the Stochastic Model for the Population Number

The differential equation for the stochastic model describing the population number which we derived in the text is:

$$\frac{dV_N}{dt} = C \binom{N+1}{2} V_{N+1} - C \binom{N}{2} V_N \quad (2.10)$$

For an initial distribution of  $N_0$  particles of unit mass we have the initial conditions:

$$V_{N_0} = 1$$

$$V_N = 0 ; N \neq N_0$$

We define a vector  $\underline{V}$  and a matrix  $\underline{M}$  as follows:

$$\underline{V} = \begin{bmatrix} V_1 \\ V_2 \\ \vdots \\ V_{N_0} \end{bmatrix}$$

$$\underline{M} = \begin{bmatrix} \binom{1}{2} & \binom{2}{2} & 0 & 00 \dots 0 \\ 0 & \binom{2}{2} & \binom{3}{2} & 00 \dots 0 \\ \vdots & \vdots & \vdots & \ddots \vdots \end{bmatrix}$$

The set of equations described by eq. (2.10) can then be written in matrix form:

$$\frac{d\underline{V}}{dt} = \underline{M}\underline{V} \quad (2.29)$$

where the eigenvalues of  $\underline{M}$  are  $\lambda_k = \binom{k}{2}$  and the characteristic vectors of  $\underline{M}$  are obtained from

$$\underline{M} \underline{X}_k = -\lambda_k \underline{X}_k \quad (2.30)$$

Equation (2.29) has particular solutions of the form

$$\underline{v}(t) = e^{-\lambda_k t'} \underline{x}_k \quad (2.31)$$

where  $t' = Ct$

Since the eigenvalues are distinct, the characteristic vectors are linearly independent. Therefore, the complete solution for the vector  $\underline{v}$  will be the sum of the particular solutions, each of which corresponds to a characteristic vector.

$$\underline{v}(t) = \sum_k c_k e^{-\lambda_k t'} \underline{x}_k \quad (2.32)$$

From (2.31) we can obtain a particular solution for one of the elements of the  $\underline{v}$  vector

$$v_N(t) = e^{-\lambda_k t'} x_{k,N} \quad (2.33)$$

Substituting (2.33) into (2.10) we obtain

$$-\lambda_k x_{k,N} = -\binom{N}{2} x_{k,N} + \binom{N+1}{2} x_{k,N+1} \quad (2.34)$$

Therefore,

$$x_{k,N+1} = \frac{\binom{N}{2} - \lambda_k}{\binom{N+1}{2}} x_{k,N} \quad (2.35)$$

and

$$x_{k,N} = \frac{\binom{N-1}{2} - \lambda_k}{\binom{N}{2}} \cdot \frac{\binom{N-2}{2} - \lambda_k}{\binom{N-1}{2}} \cdots \frac{\binom{1}{2} - \lambda_k}{\binom{2}{2}} x_{k,1}$$

If we set  $x_{k,1} = 1$  we obtain  $x_{k,N}$  in closed form:

$$x_{k,N} = \frac{N}{(N!)^2} \prod_{\gamma=1}^{N-1} \left[ \gamma(\gamma-1) - k(k-1) \right] \quad (2.36)$$

We premultiply and postmultiply both sides of (2.30) by  $\underline{Y}_j$  where  $\underline{Y}_j$  is the reciprocal vector to  $\underline{X}_k$ . Therefore,

$$\underline{Y}_j M \underline{X}_k \underline{Y}_j = -\lambda_k \underline{Y}_j \underline{X}_k \underline{Y}_j$$

$$\text{and } \underline{Y}_k M = -\lambda_k \underline{Y}_k \quad (2.37)$$

We proceed to solve for  $y_{k,N}$ . Eqn. (2.38) can be written in the form

$$\begin{bmatrix} y_{k,1} & y_{k,2} & \cdots & y_{k,N} \end{bmatrix} \begin{bmatrix} -\binom{1}{2} & \binom{1}{2} & 0 & 0 & \cdots \\ 0 & -\binom{2}{2} & \binom{3}{2} & 0 & \cdots \\ \vdots & \vdots & \vdots & \vdots & \vdots \end{bmatrix} = \lambda_k \begin{bmatrix} y_{k,1} & y_{k,2} & \cdots & y_{k,N} \end{bmatrix}$$

which yields the following system of equations

$$\begin{aligned} -\binom{1}{2} y_{k,1} &= -\lambda_k y_{k,1} \\ \binom{2}{2} y_{k,1} - \binom{2}{2} y_{k,2} &= -\lambda_k y_{k,2} \end{aligned}$$

We solve the equations to obtain  $y_{k,N}$

$$\begin{aligned} \left[ \binom{1}{2} - \lambda_k \right] y_{k,1} &= 0 \\ \vdots \\ \left[ \binom{n}{2} - \lambda_k \right] y_{k,n} &= \binom{n}{2} y_{k,n-1} \end{aligned}$$

and

$$y_{k,N} = \frac{\binom{N}{2}}{\binom{N}{2} - \binom{k}{2}} \cdot \frac{\binom{N-1}{2}}{\binom{N-1}{2} - \binom{k}{2}} \cdots$$

since

$$\lambda_k = \binom{k}{2}$$

Since the denominator can't be zero,  $y_{k,k}$  is the first non-zero term and

$$y_{k,N} = \frac{\binom{N}{2}}{\binom{N}{2} - \binom{k}{2}} \cdot \frac{\binom{N-1}{2}}{\binom{N-1}{2} - \binom{k}{2}} \cdots \frac{\binom{k+1}{2}}{\binom{k+1}{2} - \binom{k}{2}} y_{k,k} \quad (2.38)$$

Rearranging and setting  $y_{k,k} = 1$  yields

$$y_{k,N} = \frac{N!}{k!} \frac{(N-1) \cdots 1}{(k-1) \cdots 1} \prod_{v=k+1}^N \left( \frac{1}{v(v-1) - k(k-1)} \right) \quad (2.39)$$

When  $t=0$  (2.32) becomes

$$v(0) = \sum_j c_j \underline{x}_j .$$

Dotting through by  $\underline{y}_k$

$$(\underline{y}_k, v(0)) = c_k (\underline{y}_k, \underline{x}_k) \quad (2.40)$$

since

$$(\underline{y}_k, \underline{x}_j) = 0 .$$

We can now solve for  $c_k$

$$c_k = \frac{(\underline{y}_k, v(0))}{(\underline{y}_k, \underline{x}_k)} \quad (2.41)$$

and substitution of this equation into (2.32) for an element of  $\underline{v}(t)$  yields:

$$v_N(t) = \sum_k \frac{(\underline{y}_k, v(0))}{(\underline{y}_k, \underline{x}_k)} e^{-\lambda k t} \underline{x}_{k,N} \quad (2.42)$$

For our initial size distribution consisting of  $N_0$  particles of unit mass, the three vectors on the right hand side of (2.42) will be of the forms

$$v(0) = \begin{bmatrix} 0 \\ 0 \\ \vdots \\ 0 \\ 1 \\ 0 \\ 0 \\ 0 \end{bmatrix}; \quad x_k = \begin{bmatrix} 1 \\ x_{k,2} \\ \vdots \\ x_{k,k} \\ 0 \\ \vdots \end{bmatrix}; \quad y_k = \begin{bmatrix} 0 & \dots & 0 & 1 & y_{k,k+1} & \dots & y_{k,N_0} \end{bmatrix}$$

Therefore

$$(y_k, v(0)) = y_{k,N_0}$$

and

$$(y_k, x_k) = \lambda_{k,k}$$

Equation (2.42) therefore becomes

$$v_N(t) = \sum_{k=N}^{N_0} \frac{y_{k,N_0}}{\lambda_{k,k}} e^{-\lambda_k t} \lambda_{k,N} \quad (2.43)$$

where  $x_{k,k}$  and  $x_{k,N}$  are defined in (2.37) and  $y_{k,N_0}$  is defined in (2.38). Note that the limits on the summation are taken from  $N$  instead of from 1 since  $x_{k,N} = 0$  for  $k < N$ .

Substitution of (2.37) and (2.39) into (2.43) yields:

$$v_N(t) = \sum_{k=N}^{N_0} \frac{N_0! (N_0-1) \dots e^{-c \binom{k}{2} t}}{N! (N-1) \dots \prod_{\substack{\nu=N \\ \nu \neq k}}^{N_0} [\nu(\nu-1) - k(k-1)]}$$

which becomes after a few simple mathematical manipulations

$$v_N(t) = \sum_{k=N}^{N_0} \frac{(-1)^{k+N} (2k-1)(k+N-2) \dots}{N! (N-1) \dots (k-N) \dots} \prod_{\nu=1}^{k-1} \left( \frac{N_0 - \nu}{N_0 + \nu} \right) e^{-c \binom{k}{2} t} \quad (2.44)$$

The mean number of particles is

$$\langle N(t) \rangle = \sum_{N=1}^{N_0} N v_N(t)$$

Therefore,

$$\langle N(t) \rangle = \sum_{N=1}^{N_0} \sum_{k=N}^{N_0} \frac{(-1)^{k+N} (2k-1) (k+N-2)!}{[(N-1)!]^2 (k-N)!} \prod_{\nu=1}^{k-1} \left( \frac{N_0 - \nu}{N_0 + \nu} \right) e^{-c \binom{k}{2} t} \quad (2.45)$$

It can be shown that (2.45) is the same as

$$\langle N(t) \rangle = \sum_{k=1}^N (2k-1) \prod_{\nu=1}^{k-1} \left( \frac{N_0 - \nu}{N_0 + \nu} \right) e^{-c \binom{k}{2} t}$$

APPENDIX BThe Solution to Eq. (2.2)

We shall now show here that

$$V(N, x_1, x_2, \dots, t) = \varphi(x_1, x_2, \dots, x_N/N) V_N(t) \quad (2.21)$$

satisfies the differential equation

$$\begin{aligned} & dv(N, x_1, x_2, \dots; t) / dt \\ &= C \sum_k V(N+1, x_1, x_2, \dots, x_k+2, \dots, \\ & \quad x_{2k}-1, \dots; t) \binom{x_k+2}{2} \\ &+ C \sum_{j < k} \sum v(N+1, x_1, x_2, \dots, x_j+1, \dots, \\ & \quad x_k+1, \dots, x_{j+k}-1, \dots; t) \binom{x_j+1}{2} \binom{x_k+1}{2} \\ & \quad - Cv(N, x_1, x_2, \dots; t) \binom{N}{2} \end{aligned} \quad (2.2)$$

We begin by multiplying

$$\frac{dv_N}{dt} = c \binom{N+1}{2} v_{N+1} - c \binom{N}{2} v_N$$

[Eq. (2.10)] by  $\varphi(x_1, x_2, \dots, x_{N_0}/N)$ . Accordingly,

$$\begin{aligned} d \left[ v_N \varphi(x_1, x_2, \dots, x_{N_0}/N) \right] / dt \\ = c \binom{N+1}{2} v_{N+1} \varphi(x_1, x_2, \dots, x_{N_0}/N) \\ - c \binom{N}{2} v_N \varphi(x_1, x_2, \dots, x_{N_0}/N) \end{aligned} \quad (2.49)$$

and we shall now show that (2.49) is identical to (2.2);

hence, it will follow that  $\varphi(x_1, x_2, \dots, x_{N_0}/N) v_N(t)$

satisfies (2.2).

Using ea. (2.2), ea. (2.49) becomes

$$\begin{aligned} dV(x_1, x_2, \dots; t) / dt = -c \binom{N}{2} V(x_1, x_2, \dots; t) \\ + c \binom{N+1}{2} \varphi(x_1, x_2, \dots, x_{N_0}/N) v_{N+1} \end{aligned} \quad (2.50)$$

Eq. (2.2), on the other hand, can be written

$$\begin{aligned}
 dV(x_1, x_2, \dots; t) / dt &= c \binom{N}{2} V(x_1, x_2, \dots, x_{N_0}) \\
 &+ c v_{N+1} \left[ \sum_j x_{2j+2} \varphi(x_1, x_2, \dots, x_{j+2}, \dots, \right. \\
 &\quad \left. x_{2j-1}, \dots, x_{N_0/N+1} \right) \\
 &+ \sum_{k < \ell} \sum (x_k+1)(x_\ell+1) \varphi(x_1, x_2, \dots, x_k+1, \dots, \\
 &\quad \left. x_\ell+1, \dots, x_{k+\ell-1}, \dots, x_{N_0/N+1} \right) \quad (2.51)
 \end{aligned}$$

To show that eas. (2.50) and (2.51) are identical, we need only show that the coefficients of  $v_{N+1}$  in both equations are the same.

Accordingly, using the expression for  $\varphi(x_1, x_2, \dots, x_{N_0}/N)$  of (2.22), we have to demonstrate that

$$\begin{aligned}
 &\frac{(N+1)!N! (N_0-N)!}{2x_1!x_2!\dots x_{N_0}! (N_0-1)!} \\
 &= \frac{(N+1)!N! (N_0-N-1)!}{2(N_0-1)!} \\
 &\quad \times \sum_j \frac{1}{x_1!x_2!\dots x_{2j-1}! (x_{2j-1})!(x_{2j-1})!\dots x_{N_0}!} \\
 &\quad + \frac{(N+1)!N! (N_0-N-1)!}{(N_0-1)!} \\
 &\quad \times \sum_{k < \ell} \sum \frac{1}{x_1!x_2!\dots (x_{k+\ell-1})!\dots x_{N_0}!}
 \end{aligned}$$

Combining the two terms on the right hand side, we obtain

$$\frac{(N_0 - N)!}{x_1! \dots x_{N_0}!} = (N_0 - N - 1)! \sum_k \sum_l \frac{1}{x_1! x_2! \dots (x_{k+l} - 1)! \dots x_{N_0}!} \binom{x_{k+l}}{x_{k+l}}$$

which reduces to

$$\frac{(N_0 - N)!}{x_1! x_2! \dots x_{N_0}!} = \frac{(N_0 - N - 1)!}{x_1! x_2! \dots x_{N_0}!} \sum_k \sum_l x_{k+l}$$

Noting that

$$\sum_k \sum_l x_{k+l} = N_0 - N,$$

we find that the two sides are indeed, identical and we have therefore demonstrated that eq. (2.21) satisfies the differential equation (2.2).

## BIBLIOGRAPHY

1. Berg, J.G., Owe, J.C., Clutter, J.A. Gaukler, and R.J. McDonald. 1968: Conversion of water vapor to ice by silver iodide. J. Atmos. Sci., 25, 464-469.
2. Bergeron, J. 1935: On the physics of cloud and precipitation. Process-Verb. Assoc Met U.GPG.I. Part 2, 156-178.
3. Berry, E.X., 1967: Cloud droplet growth by collection. J. Atmos. Sci., 24, 688-701.
4. Berry, E.X., 1968: Comments on "Cloud droplet coalescence: Statistical foundations and a one-dimensional sedimentation model." J. Atmos. Sci., 25, 151-152.
5. Braham, R.R., Jr. and J.R. Sievers, 1955: Overseeding of cumulus clouds. Conf. on Cloud Physics of Cloud and Precipitation Particles, 7-10 Sept. 1955, Woods Hole, Mass., 250-265.
6. Byers, H.R. 1965: Elements of cloud physics. Univ. of Chicago Press.
7. Danielson, E.F., R. Bleck and D.A. Morris, 1972: Hail growth by stochastic collection in a cumulus cloud. J. Atmos Sci., 29, 135-154.
8. Drake, R.L. 1972: The scalar transport equation of coalescence theory: Moments and kernels. J. Atmos. Sci., 29, 537-547.

9. Feller, W., 1967: An Introduction to Probability Theory and its Applications, Vol. 1, 3rd ed. New York, Wiley.
10. Gillespie, D.N., 1972: The stochastic coalescence model for cloud droplet growth. J. Atmos. Sci., 29, 1496-1510.
11. Golovin, A.M., 1963: The solution of the coagulation equation for cloud droplets in a rising air current. Bull. (Izv.) Acad. Sci. USSR. Geophys. Ser., 482-87.
12. Golovin, A.M., 1965: Kinetics of cloud droplets in a model of stationary axisymmetrical cumulus clouds. Bull. (Izv.) Acad. Sci. USSR. Geophys. Ser., 422-426.
13. Hindman, E.E. II. and D.B. Johnson, 1972: Numerical simulation of ice particle growth in a cloud of super-cooled water droplets. J. Atmos. Sci., 29, 1313-1321.
14. Hosler, C.L. and R.E. Hallgren, 1960: The aggregation of small ice crystals. Far. Soc. Trans., 30, 200-207.
15. Hulburt, H.M. and S. Katz, 1964: Some problems in particle technology. Chem. Eng. Sci., 19, 555-574.
16. Hulburt, H.M., M.H. Bayewitz and R. Shinnar (1975). In preparation.
17. Kapur, P.C. and D.W. Fuerstenau, 1969: A coalescence model for granulation. Ind. Eng. Chem. Process Develop., 8, 55-62.

18. Katz, S. and R. Shinnar, 1969: Probability methods in particulate systems. Ind. Eng. Chem., 61, 60-73.
19. Klepfer, J.S., R. M. Sonshine, and R. Shinnar, 1969: A nucleation model for the polymerization of precipitating polymers in aqueous solutions. AICHE Symposium, Cleveland, Ohio, 4-7 May 1969.
20. Knight, B.B., 1971: Some condensation processes of McKean Type. J. Appl. Prob., 8, 399-406.
21. Knutson, E.O., K. W. Pontinen and L. W. Rees, 1967: Coagulation in ten-micron aerosols. Amer. Ind. Hyg. Assoc. J., 28, 83-89.
22. Koenig, L.R., 1966: Numerical test of validity of the drop-freezing/splintering hypothesis of cloud glaciation. J. Atmos. Sci., 23, 727-740.
23. Long, A. B., 1971: Validity of the finite-difference droplet collection equation. J. Atmos. Sci., 28, 210-217.
24. Long, A. B., 1972: Reply (to Scott). J. Atmos. Sci., 29, 594-595.
25. Marcus, A.H., 1968: Stochastic Coalescence. Technometrics, 10, No. 1, 133-143.
26. Ryan, B. F., 1973: A numerical study of the nature of the glaciation process. J. Atmos. Sci., 30, 824-834.
27. Saffman, P. G. and J. S. Turner, 1956: On the collision of drops in turbulent clouds. J. Fluid Mechanics, 1, 16-30.

28. Scott, W. T., 1967: Poisson statistics in distributions of coalescing droplets, J. Atmos. Sci., 24, 221-225.
29. Scott, W. T., 1968: Analytic studies of cloud droplet coalescence I. J. Atmos. Sci., 25, 54-65.
30. Scott, W. T., 1968: Comments on "Cloud droplet coalescence: Statistical foundations and a one-dimensional sedimentation model." J. Atmos. Sci., 25, 150.
31. Scott, W. T., 1972: Comments on "Validity of the finite-difference droplet collection equation." J. Atmos. Sci., 29, 593-594.
32. Simpson, J., R. H. Simpson, D. A. Andrews, and M. A. Eaton, 1965: Experimental cumulus dynamics. Rev. Geophys. 3:3, 387-431.
33. Slinn, W. G. N., 1971: Time constant for cloud seeding and tracer experiments. J. Atmos. Sci., 28, 1509-1511.
34. Slinn, W. G. N., and A. G. Gibbs, 1971: The stochastic growth of a rain droplet. J. Atmos. Sci., 28, 973-981.
35. Stalevich, D. D. and T. S. Uchevatkina, 1967: Optimum dosages of ice forming agents used in cloud seeding to produce precipitation. USSR Glavnaia Geofizicheskaiia Observaoriia, Leningrad, Trudy, No. 202: 13-21.

36. Takeda, T., 1968: Solid precipitation in a super-cooled cloud: Part 2 - Growth of a solid precipitation particle. J. Meteor. Soc., Japan, 46, 255-264.
37. Twomey, S., 1966: Computations of rain formation by coalescence. J. Atmos. Sci., 23, 405-411.
38. Warshaw, M., 1967: Cloud droplet coalescence: Statistical foundation and a one-dimensional sedimentation model. J. Atmos. Sci., 24, 278-286.
39. Warshaw, M., 1968: Reply (to Scott). J. Atmos. Sci., 25, 152-154.
40. Weickmann, R. K., U. Katz and R. Steele, 1970: Silver iodide-sublimation or contact nucleus? Pre-prints of papers, Second National Conf. Weather Modification, Santa Barbara, Calif., Amer. Meteor. Soc., 332-336.

## VITA

Marvin H. Bayewitz was born in Brooklyn, New York on May 3, 1947. He received his elementary and high school education at local Jewish Day Schools. He attended Brooklyn College for two years as a pre-engineering student and subsequently transferred to the City College of New York where he received his Bachelor's Degree in Chemical Engineering (June 1969, Cum Laude) and his Master's Degree in Chemical Engineering (June 1971). During the summers of 1967-1970 the author was involved in research and development at Esso Research and Engineering Company, Eastern Kodak Company, Technion University (Israel), and Monsanto Company. The author held a National Science Foundation Traineeship at City College (1969-1973) where he was engaged in Doctoral research in the course of which he has published a paper in the field of Coalescence. Since December 1973, the author has held a position at Bethlehem Steel Corporation where he is involved in process control. Marvin Bayewitz is married to Passi Rosen and lives in Highland Park, New Jersey. He plans a career in research and development.